1   **Running Title:** Cloning of a kernel size QTL in maize

2

3   **Correspondence to**: Jianbing Yan (email: yjianbing@mail.hzau.edu.cn) and David Jackson

4   (jacksond@cshl.edu)

5   Tel: +86 27 87280110

6   National Key Laboratory of Crop Genetic Improvement, No.1 Shizishan Street, Hongshan

7   District, Wuhan, Hubei 430070, China.

8

9   **Article title**

10   *qKW9* encodes a pentatricopeptide repeat protein affecting photosynthesis and grain filling in

11   maize

12   **Authors**

13   Juan Huang[1], Gang Lu[1], Lei Liu[1,2], Mohammad Sharif Raihan[1], Jieting Xu[1,3], Liumei Jian[1],

14   Lingxiao Zhao[4,5], Thu M. Tran[2,6], Qinghua Zhang[1], Jie Liu[1], Wenqiang Li[1], Cunxu Wei[4], David

15   M. Braun[6], Qing Li[1], Alisdair R. Fernie[7], David Jackson[1,2,*], Jianbing Yan[1,*]

16

17   [1]National Key Laboratory of Crop Genetic Improvement, Huazhong Agricultural University,

18   Wuhan 430070, China

19   [2]Cold Spring Harbor Laboratory, Cold Spring Harbor, NY, USA.

20   [3]Wimi Biotechnology Co., Ltd, 4th Floor, Kejizhuanhua building, No. 3 Meishan Road,

21   Xinbei District, Changzhou City, Jiangsu Province, China

22   [4]Jiangsu Key Laboratory of Crop Genetics and Physiology, Co-Innovation Center for Modern

23   Production Technology of Grain Crops, Yangzhou University, Yangzhou 225009, China

24   [5]Jiangsu Xuzhou Sweetpotato Research Center, Xuzhou, Jiangsu, China

25   [6]Division of Biological Sciences, Interdisciplinary Plant Group, Missouri Maize Center,

26   University of Missouri, Columbia, MO 65211, USA

27   [7]Department of Molecular Physiology, Max-Planck-Institute of Molecular Plant Physiology,

28   Am Mühlenberg 1, 14476 Potsdam-Golm, Germany

29

One sentence summary

31 A pentatricopeptide repeat protein exerts quantitative effect on maize kernel weight and size

32 by affecting photosynthesis and grain filling.

33

40

49 **Competing financial interests**

50 The authors declare no competing financial interests.

51 **Abstract (<250 words)**

52 Kernel weight is an important yield component in maize that was selected during

53 domestication. Many kernel weight genes have been identified through mutant analysis, and

54 are mostly involved in the biogenesis and functional maintenance of organelles or other

55 fundamental cellular activities. However, only a limited number of loci underlying quantitative

56 variation in kernel weight have been cloned. Here we characterize a maize kernel weight QTL,

57   *qKW9* and find that it encodes a DYW motif pentatricopeptide repeat protein involved in

58   C-to-U editing of NdhB, a subunit of the chloroplast NADH dehydrogenase-like complex. In a

59   null *qKW9* background, C-to-U editing of NdhB was abolished, and photosynthesis was

60   reduced, suggesting that *qKW9* regulates kernel weight by controling the maternal source of

61   photosynthate for grain filling. Characterization of *qKW9* highlights the importance of

62   optimizing photosynthesis on maize grain yield production.

63   **Keywords**

64   Kernel weight; maize yield; QTL; photosynthesis; Cyclic electron transport; C-to-U editing;

65   NDH complex

66

67   **INTRODUCTION**

68   Maize (*Zea mays*) is one of the most important crops in the world, producing grain vital for

69   our survival. Along with population growth, environmental deterioration, the decline of arable

70   land and climate change challenge us to increase maize grain production. Therefore, the

71   improvement of maize yield is of great importance to the sustainable development of human

72   society.

73   The grain yield of maize is comprised of several components, including ear number per

74   plant, kernel number per cob, and kernel weight. As an essential yield component, kernel

75   weight is positively correlated with yield, and is determined during development by kernel

76   size and the degree of kernel filling (Scanlon and Takacs, 2009). To dissect the genetic

77   architecture of maize kernel weight, numerous studies have identified hundreds of

78   quantitative trait loci (QTL) for kernel traits (www.maizegdb.org/qtl). However, only a few

79   kernel size QTL have been cloned and studied, and some maize kernel weight genes have

80   been identified as homologs of rice genes(Li et al., 2010a; Li et al., 2010b; Liu et al., 2015).

81   In one large-scale QTL study in maize, 729 QTL regulating kernel weight-related traits were

82   identified, and 24 of 30 genes were in, or tightly linked to, 18 rice grain size genes, suggesting

83   conserved genetic architecture of kernel weight(Liu et al., 2017b). One example is *teosinte*

84   *glume architecture1* (*tga1*), the causal gene underlying the change from encased kernels in

85   the wild progenitor teosinte to naked kernels in maize(Wang et al., 2005; Wang et al., 2015).

86   Reducing expression of *tga1* in maize by RNAi greatly increases kernel size and weight,

87   suggesting that the removal of glumes from teosinte could release growth constraints, and

88   provide more space to allow larger kernels to develop (Wang et al., 2015). Another kernel

89   size gene, *ZmSWEET4c*, affects kernel weight in a different manner, with its product

90   mediating sugar transport across the basal endosperm transfer cell layer, and shows signals of

91   selection during domestication (Sosso et al., 2015). Recently a further gene, *BARELY ANY*

92   *MERISTEM1d* (*ZmBAM1d*) was identified as an additional QTL responsible for kernel weight

93   variation in maize (Yang et al., 2019).

94   Despite limited progress on our understanding of the quantitative variation in maize

95   kernel weight, numerous kernel mutants have been identified (Neuffer and Sheridan, 1980;

96   Clark and Sheridan, 1991). These mutants have been grouped into three categories: (i)

97   defective kernel (*dek*) mutations, including empty pericarp (*emp*) mutants that affect both

98   endosperm and embryo; (ii) embryo-specific (*emb*) mutations with healthy endosperm

99   formation; and (iii) endosperm-specific mutations (McCarty, 2017). Mutants in categories i

100   and ii have detrimental effects, leading to significant loss of kernel weight. Several of these

101   maize kernel development genes have been identified. For instance, *EMP10*(Cai et al., 2017),

102   *EMP11* (Ren et al., 2017), *EMP12* (Sun et al., 2019), *EMP16* (Xiu et al., 2016), *DEK35* (Chen

103   et al., 2017)*,* and *DEK37* (Dai et al., 2018) are involved in intron splicing of mitochondrial

104   genes. In contrast, *MPPR6* functions in maturation and translation initiation of mitochondrial

105   ribosomal protein subunit mRNA(Manavski et al., 2012). Mutations of these genes impair

106   mitochondral function, leading to defective kernels. Other genes, including *EMP7* (Sun et al.,

107   2015), *DEK10* (Qi et al., 2017), *DEK39* (Li et al., 2018), *PPR2263/MITOCHONDRIAL*

108   *EDITING FACTOR29* (Sosso et al., 2012), and *SMALL KERNEL1* (Li et al., 2014) function in

109   C-to-U editing of transcripts in mitochondria and chloroplasts.

110   Many kernel size genes encode pentatricopeptide repeat (PPR) proteins, a large family

111   of RNA-binding proteins in land plants, with more than 400 members in *Arabidopsis*

112   (*Arabidopsis thaliana*), rice (*Oryza sativa*), and maize (*Zea mays*) (Lurin et al., 2004;

4

113 Schmitz-Linneweber and Small, 2008; Barkan and Small, 2014). Members of the PPR family

114 are characterized by tandem arrays of a degenerate 35-amino-acid motif (PPR motif), and the

115 PPR family is divided into P and PLS subfamilies, according to the nature of the PPR motifs.

116 Members of the P subfamily function in various processes of RNA maturation in organelles,

117 including RNA stabilization, splicing, intergenic RNA cleavage, and translation (Barkan and

118 Small, 2014). The PLS subfamily contains canonical PPR (P) motifs, as well as long (L) and

119 short (S) PPR-like motifs, in a P-L-S pattern. This subfamily is further divided into PLS,

120 E/E+, and DYW classes, based on their C-terminal domains (Barkan and Small, 2014). PLS

121 subfamily members function in RNA editing (Barkan and Small, 2014), a post-transcriptional

122 modification of organelle transcripts, including C-to-U, U-to-C and A-to-I editing

123 (Chateigner-Boutin and Small, 2010; Ruwe et al., 2013; Ruwe et al., 2019).

124   Kernel size and carbohydrate import into kernels directly determine the grain yield of

125 maize, therefore, elucidation of the genetic basis of kernel traits could provide favorable

126 alleles to enhance maize breeding. In a previous study, a maize recombinant inbred line (RIL)

127 population was developed from a cross between two diverse parents, Zheng58 and SK (Small

128 Kernel), which show dramatic variation in kernel weight; and a major kernel weight QTL,

129 *qKW9,* was identified (Raihan et al., 2016; Yang et al., 2019). In this study, we mapped and

130 cloned the causative gene underlying *qKW9,* and identified it as a PLS-DYW type PPR protein.

131 We found that qKW9 is required for C-to-U editing at position 246 of *NdhB*, a

132 chloroplast-encoded subunit of the NDH complex. Functional characterization revealed that

133 C-to-U editing of *NdhB* is crucial for the accumulation of its protein product as well as the

134 activity of the NDH complex. Impairment of this complex led to lower photosynthetic

135 efficiency and a corresponding yield loss of maize in field trials.

136

137   **RESULTS**

138   **Fine mapping and validation of *qKW9***

139   *qKW9* is a major QTL regulating maize kernel weight identified in the ZHENG58×SK RIL

140   population (Raihan et al., 2016). Near-isogenic lines (NILs) harboring the *qKW9* allele from

141   SK or ZHENG58 were screened from RIL-derived heterogeneous inbred families (HIFs) and

142   used to fine map *qKW9*. In contrast to *dek* mutants, which have dramatic kernel weight loss

143   due to defects in the embryo and/or endosperm, the NIL-SK kernels weighed only about 3g

144   less per hundred kernels, compared to NIL-ZHENG58, and their kernel morphology, starch

145   granule structure and plant morphology were similar (Figure 1, Table S1). Thus, the kernel

146   development of NIL-SK plants was not strongly affected. Interestingly, two-week-old

147   seedlings of NIL-SK were smaller than NIL-ZHENG58, possibly as a result of less nutrition

148   from smaller kernels for their heterotrophic growth (Figure1B). However, at the mature stage,

149   NIL-SK, and NIL-ZHENG58 plants had similar plant architecture(Figure 1A and 1C).

150   NIL-SK plants had the same kernel row number but fewer kernels per row compared to

151   NIL-ZHENG58 plants , resulting in smaller ears with fewer kernels (Figure 1D and Table 1).

152   In previous study, line KQ9-HZAU-1341-1 from ZHENG58×SK RIL population with

153   residual heterozygosity was used as founder line to fine map qKW9.2(Raihan et al., 2016; Liu

154   et al., 2018). After three generations self-cross and screening against descendents of

155   KQ9-HZAU-1341-1, several recombinant HIFs were obtained. Among the HIFs, F1H5 was

156   used to generate recombination populations to screen for new recombinants to fine map *qKW9*

157   in this study. Eight recombinants was identified by screening 685 F1H5 descendents and they

158   were self-crossed for further analysis (Figure S1). By comparing Hundred Kernel Weight

159   (HKW) of the homozygous progenies from all recombinants, *qKW9* was fine mapped to a ~

160   20kb region defined by markers M3484 and M3506 (156.65Mb and 156.67Mb, respectively in

161   B73 RefGen v4) (Figure 2A and Fig S1). Three genes (*Zm00001d04850*, *Zm00001d048451*,

162   and *Zm00001d048452*) were annotated within this region in B73 RefGen v4 (Figure 2B).

163   Several SNPs were found in Zm00001d04850, however they were all synonymous. The second

164   gene, Zm00001d048451, had a 13bp-CDS-deletion in SK, possibly leading to loss of function
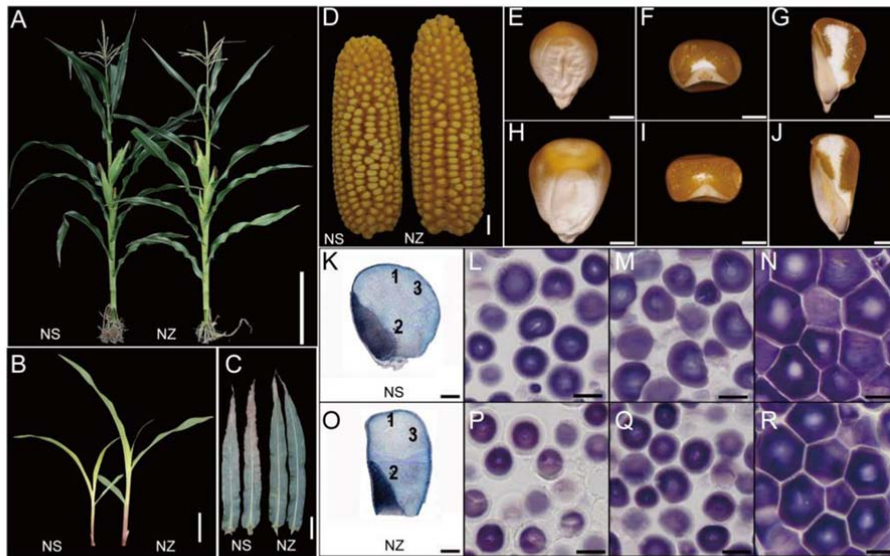
Figure 1. Plant and kernel morphology of NIL-SK and NIL-Zheng58. **(A)** NIL-SK (NS) and NIL-Zheng58 (NZ) had very similar plant architecture, Bar=20cm. **(B)** NIL-SK (NS) two-week old seedlings were smaller than NIL-Zheng58 (NZ). Bar=4cm. **(C)** Leaf senescence was greater in NIL-SK (NS) at 30 days after pollination compared to NIL-Zheng58. Bar=10cm. **(D)** Ears of NIL-SK (NS) were smaller than in NIL-Zheng58 (NZ). Bar=1cm. **(E) to (J)** Mature kernels of NIL-SK (E-G) were smaller that in NIL-Zheng58 (H-J). Whole kernels of NIL-SK and NIL-Zheng58 (**[E]** and **[H]**). Bar=2mm; transverse section of kernel of NIL-SK and NIL-Zheng58(**[F]** and **[I]**). Bar=2mm; Longitudinal section of kernel of NIL-SK and NIL-Zheng58(**[G]** and **[J]**). Bar=2mm; **(K) to (R)** Similar starch structure in endosperms of mature kernels of NIL-SK and NIL-Zheng58. Whole longitudinal section stained with iodine solution of kernels of NIL-SK and NIL-Zheng58 (**[K]** and **[O]**), 1, 2, 3 indicate the crown, farinaceous and keratin endosperm regions, respectively. Bar=1mm; **(L)** to **(N)** correspond to regions 1, 2, 3 in **(K)**; and **(P)** to **(R)** correspond to regions 1, 2, 3 in **(O)**. Bar=10μm.

165 (Figure 2C). We failed to amplify the third gene, *Zm00001d048452*, from both SK and

166 ZHENG58, and therefore, screened SK and ZHENG58 BAC libraries to search for sequence

167 variation. However, sequence alignment and annotation revealed that *Zm00001d048452* was

168 absent from both SK and ZHENG58, and there were no additional annotated genes within the

169 *qKW9* locus, although there were some large-fragment insertions or deletions in the intergenic

170 regions (Figure 2B). These results were further verified using the assembled SK genome (Yang

171 et al., 2019). Of the two remaining candidates, *Zm00001d048450* displayed neither change in

172 expression level nor pattern (Figure S2A), which together with its lack of non-synonymous

173 SNPs suggested *Zm00001d048451* to be the causative gene of *qKW9*.

174   To validate *Zm00001d048451* as the gene underlying *qKW9*, we adopted the
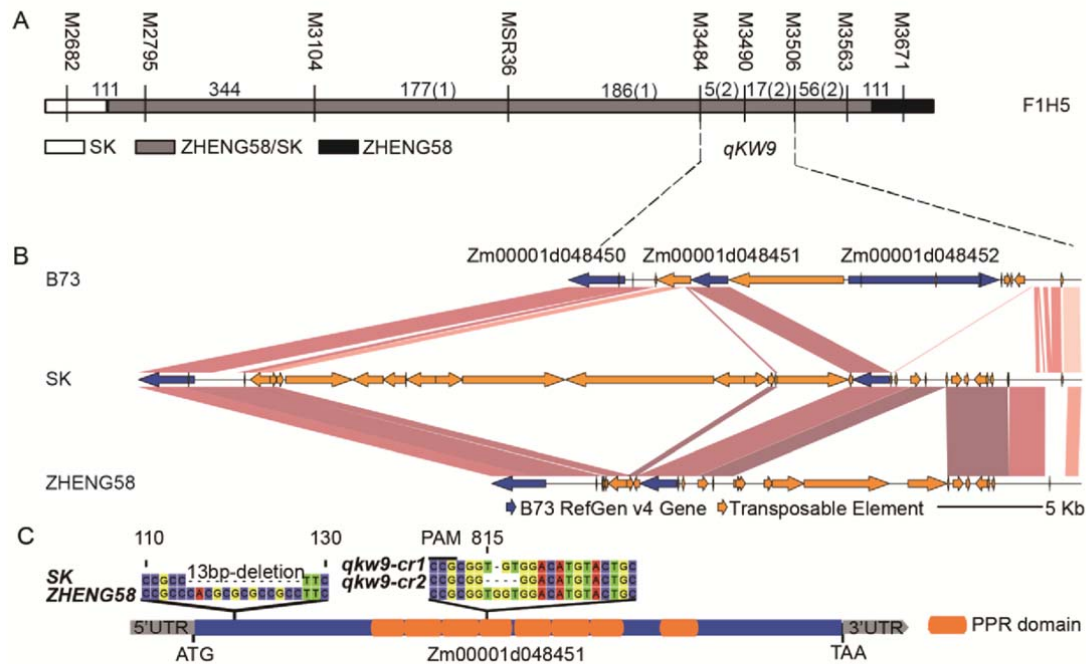
Figure 2. Fine mapping and gene structure of qKW9. **(A)** Mapping delimits *qKW9* to the region between M3484 and M3506 on chromosome 9. F1H5 which derives from ZHENG58 × SK RIL population is the founder line for screening heterozygous inbred families (HIFs) for fine mapping *qKW9*. Progeny tests of kernel weight were conducted on the resulting recombinant families. White bar represents the homozygous chromosomal segment for SK, grey bar represents the heterozygous chromosomal segment for ZHENG58 × SK, black bar represents the homozygous chromosomal segment for ZHENG58. The graphical genotype represents F1H5. Numbers between markers represent physical distances (Kb) between the adjacent markers and numbers in brackets represent the number of recombinants. **(B)** Gene annotations in the region of *qKW9* of B73, SK, and Zheng58. Sequences were obtained by sequencing BACs covering *qKW9* from SK and ZHENG58 genome BAC libraries, respectively. Zm00001d048452 was absent in both SK and ZHENG58. Two candidate genes-*Zm00001d048450* and *Zm00001d048451*- were identified in *qKW9*. **(C)** *Zm00001d048451* is a 1.8kb intron-less gene with 8 pentatricopeptide repeats and a 13bp-deletion was identified in coding region of *Zm00001d048451* in SK. CRISPR/Cas9 was used to create knockout mutants with a single guide sequence (the 20bp sequence adjacent to PAM) targeting *Zm00001d048451* in the inbred C01. Two mutated alleles - *qkw9-cr1* and *qkw9-cr2* - were identified by sequencing the first-generation (T0) plants and used for further genetic analysis.

175 CRISPR/Cas9 system to create knockout mutants (Figure 2C). Editing of *qKW9* was

176 identified by Sanger sequencing of T_0 transgenic plants, and two null mutants, *qKW9*-cr1,

177 carrying a 1bp-deletion, and *qKW9*-cr2, carrying a 4bp-deletion, were used for subsequent

178 analysis (Figure 2C and Figure 3). For both alleles, we found that kernel weight and ear

179 weight were reduced compared to their corresponding wild type (Figure 3), demonstrating

8
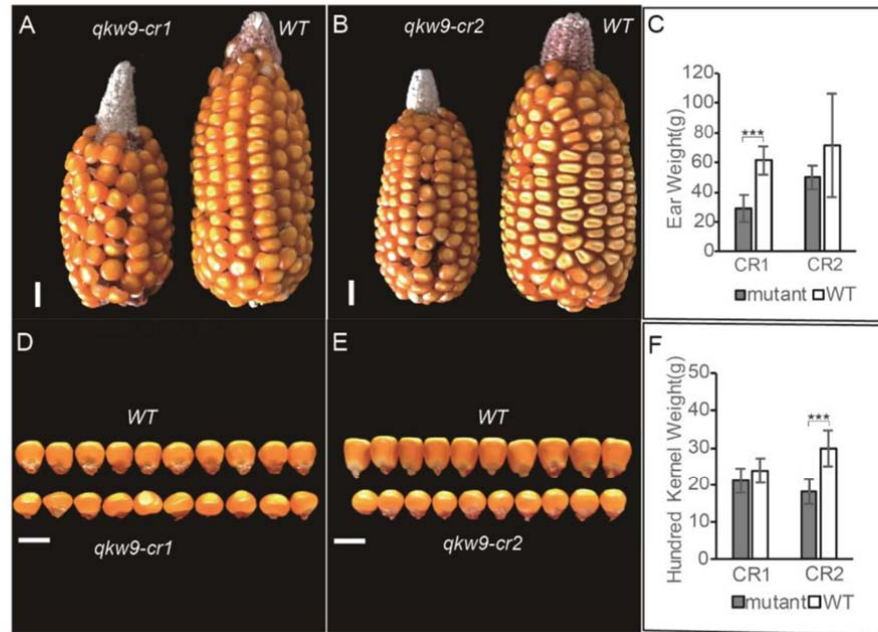
Figure 3. Two CRISPR/Cas9 knockout mutants of Zm00001d048451-*qkw9-cr1* and *qkw9-cr2*-produced smaller ears and smaller kernels than wild type. Each mutant is shown alongside its corresponding wild type segregant from a single Cas9-free T_1 generation plant. **(A)** and **(B)** comparison of ears produced by CRISPR/Cas9 mutants (left) and WT (right). *qkw9-cr1* (left) and wild type (right) in **(A)** and *qkw9-cr2* (left) and wild type (right) in **(B)**. Bar=1cm. **(D)** and **(E)** kernels produced by CRISPR/Cas9 mutants (lower row) were smaller than   WT (upper row). *qkw9-cr1* (lower) and wild type (upper) in **(D)** and *qkw9-cr2* (lower) and wild type (upper) in **(E)**. Bar=1cm. **(C)** and **(F)** show reductions in ear weight **(C)** and kernel weight **(F)** of CRISPR/Cas9 knockout mutants. Data are shown as mean ± SD (n=6). *** P < 0.001.

180   that Zm00001d048451 was indeed the causative gene of *qKW9*.

181   **qKW9 is highly expressed in leaf, and encodes a chloroplast protein involved in *NdhB***

182   **RNA editing**
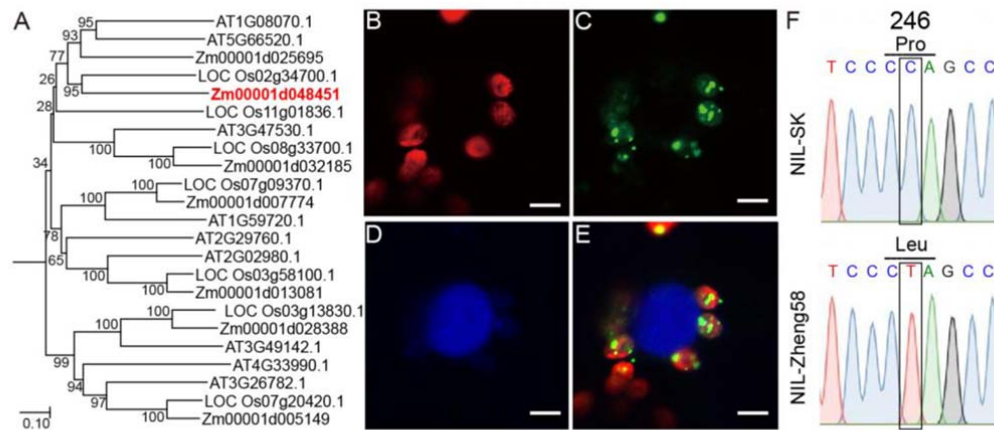
Figure 4. Characterization of *qKW9/Zm00001d048451*. **(A)** Phylogenetic tree of maize, Arabidopsis and rice PLS-E, PLE-E+, and PLS-DYW Pentatricopeptide Repeat genes predicted to localize in chloroplast/plastid by TargetP. **(B)** Autofluorescence of chlorophyll (red). **(C)** qKW9-GFP fusion protein (green) in green puncta within plastids **(D)** DAPI staining (blue) of nuclei **(E)** Overlay of **(B)**, **(C)** and **(D)**. Scale bar=5 μm. **(F)** Allele in NIL-SK of *Zm00001d048451* fails to edit C to U in 246th codon of *NdhB* gene. C-to-U editing in NdhB-246 results in amino acid change from proline to leucine. Pro, proline; Leu, leucine.

183   *Zm00001d048451/qKW9* is predicted to encode a DYW subgroup pentatricopeptide repeat

184   (PPR) protein with eight putative PPR motifs (Figure 2C). An Arabidopsis ortholog,

185   *AT5G66520* (Figure 4A) encodes a DYW subgroup protein with ten PPR motifs and was

186   designated *Chloroplast RNA Editing Factor 7* (*CREF7*), functioning in *Ndh* editing (Yagi et al.,

187   2013). In order to address if *qKW9* is also involved in chloroplast RNA editing, we analyzed its

188   expression and subcellular localization. Real-time PCR of *qKW9* revealed a considerably

189   higher expression level in leaf than in other tissues (Figure S2B). *qKW9* expression was

190   detected in all leaf-related tissues, and its expression level (13.9-87.6 FPKM) was much higher

191   than in other tissues (0-12.8 FPKM) (Stelpflug et al., 2016). To test the subcellular localization

192   of *qKW9*, we transiently expressed a *qKW9*-GFP fusion protein in tobacco, and found

193   localization in the stroma of chloroplasts (Figure4B-4E), agreeing with a chloroplast prediction

194   by TargetP (Emanuelsson et al., 2007).

195   To evaluate RNA editing by *qKW9*, leaves from NIL-SK and NIL-ZHENG58 plants

196   before and after pollination were collected for total RNA sequencing. By comparing editing

197   frequencies between NIL-SK and NIL-ZHENG58, six loci putatively edited by qKW9 were

198   identified with p-value < 0.05 and mean editing frequency difference > 5% (Table 2). Three of

199   these loci at chloroplast genome positions 90736, 132001, and 65407 (B73 RefGen v4), had

200   striking editing differences between NIL-SK and NIL-ZHENG58, with close to 100% editing

201   in NIL-ZHENG58 but almost none in NIL-SK at all stages tested (Table 2). Position 65407 is

202   in an intergenic region, whereas positions 90736 and 132001 are in the 246th codon of

203   *GRMZM5G876106* and *GRMZM5G810298,* respectively (Table 2). These genes are the two

204   copies of *NdhB* in the chloroplast genome, and their C-to-U editing changes the 246th amino

205   acid from proline to leucine. Thus, the sites edited by *qKW9* were designated as *NdhB-246*.

206   We confirmed the *NdhB-246* editing difference by Sanger sequencing in NIL-SK and

207   NIL-ZHENG58 (Figure 4F). We also investigated the editing frequency of *NdhB-246* in

208   leaves of our two CRISPR/Cas9 null mutants, as expected, *NdhB-246* editing being abolished

209   in both mutants (data not shown). These results demonstrate that *qKW9* is essential for

210   *NdhB-246* editing.

211   RNA editing defects may directly alter protein function or affect its ability to form

212   complexes with other proteins (Hammani et al., 2009). *NdhB* encodes a subunit of the NDH

213   complex (Laughlin et al., 2019), so we asked if this complex accumulates in the null *qKW9*

214   background using protein blots probed with antibodies against NdhH to monitor

215   accumulation of the complex. In NIL-SK, the level of NdhH was reduced to less than 25% of

216   NIL-ZHENG58 (Figure 5), suggesting that *NdhB-246* RNA editing by *qKW9* is important for

217   normal accumulation of the NDH complex.

218   **C-to-U editing of *NdhB-246* is essential for optimal activity of NDH complex, electron**

219   **transport rate and non-photochemical quenching induction**

220   The chloroplast NADH dehydrogenase (NDH) complex transfers electrons originating

221   from Photosystem I (PSI) to the plastoquinone pool, while concomitantly pumping protons

222   across the thylakoid membrane (Strand et al., 2017). Its activity can be monitored as a

223   transient increase in chlorophyll fluorescence, reflecting plastoquinone reduction after turning

224   off actinic light (AL) (Burrows et al., 1998; Shikanai et al., 1998). In Arabidopsis, several

225   nuclear mutants affecting NDH activity function in RNA processing of NDH subunit

226   transcripts. For instance, *Chlororespiratory Reduction 2* (*CRR2*) functions in the intergenic

227   processing of chloroplast RNA between *rps7* and *NdhB* (Hashimoto et al., 2003). A null allele

228   of *CRR2* lacks NDH activity, and the post-illumination increase in chlorophyll fluorescence is

229   undetectable, with a similar phenotype being observed in the tobacco *NdhB* mutant

230   (Hashimoto et al., 2003).

231   To check whether *qKW9* impaired NDH activity, we monitered chlorophyll fluorescence

232   using the post-illumination method (Burrows et al., 1998; Shikanai et al., 1998). Figure 6A

233   shows a chlorophyll fluorescence trace from wild-type maize and *qkw9-cr1* and *qkw9-cr2*. In

234   both *qkw9-cr1* and *qkw9-cr2*, the post-illumination increase of chlorophyll fluorescence was

235   reduced, indicating that NDH activity was diminished in the null *qKW9* background, and that

236   the Leu residue at position 246 of NdhB protein is required for NDH accumulation and

237   activity. We next measured non-photochemical quenching (NPQ), a chlorophyll fluorescence

238   parameter indicative of the level of thermal dissipation. NPQ was induced with increasing light
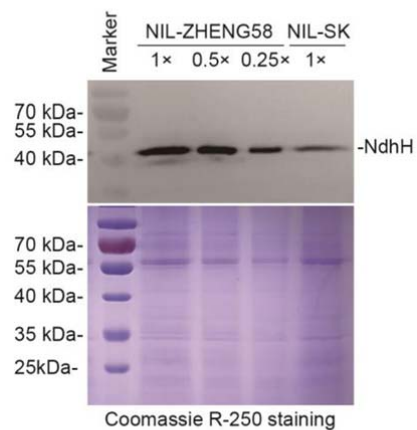
Figure 5. Protein blot analysis of the NDH complex. Chloroplast membrane protein was extracted with a commercial kit and protein samples were quantified with BCA protein assay. 1× sample amount equals 40 μg protein. Antibody against NdhH was used to indicate the amout of NDH complex. Chloroplast membrane protein from NIL-ZHENG58 was loaded a series of dilutions as indicated. Specific bands corresponded in size of NdhH protein (expected in 45 kDa, apparent in 49 kDa). Signals in NIL-ZHENG58 declined along with the dilution. The level of NdhH in NIL-SK was reduced to less than 25% of NIL-ZHENG58. Coomassie R-250 staining was used to show the proteins separated by electropheris as a loading control.

239   intensity in both *qkw9*-cr1 and wild type prior to saturation of the ETR (Figure 6B). However,

240   its induction in *qkw9*-cr1 was significantly lower at light intensities of   2413 $\mu mols^{-2}m^{-1}$,

241   indicating that thermal dissipation was impaired in *qkw9*-cr1(Figure 6B). ETR represents the

242   relative flow of electrons through PSII during steady-state photosynthesis. It increases with

243   increases in light intensity until a point at which it cannot be further increased – termed its

244   saturation point. For both wild-type and *qkw9*-cr1, the saturation point was over 400

245    $\mu mol/m^2s$ (Figure 6C). Whilst, ETR was not affected in *qkw9-cr1* at a low light intensities of

246   ~100 $\mu mols^{-2}m^{-1}$ (Figure 6C), it tended to be lower in *qkw9-cr1* at intensities above this

247   (significantly so at 200 and 2400 $\mu mols^{-2}m^{-1}$). These altered ETR activities are consistent

248   with the overall reduced grain yield in NIL-SK considering that light intensity is far in excess
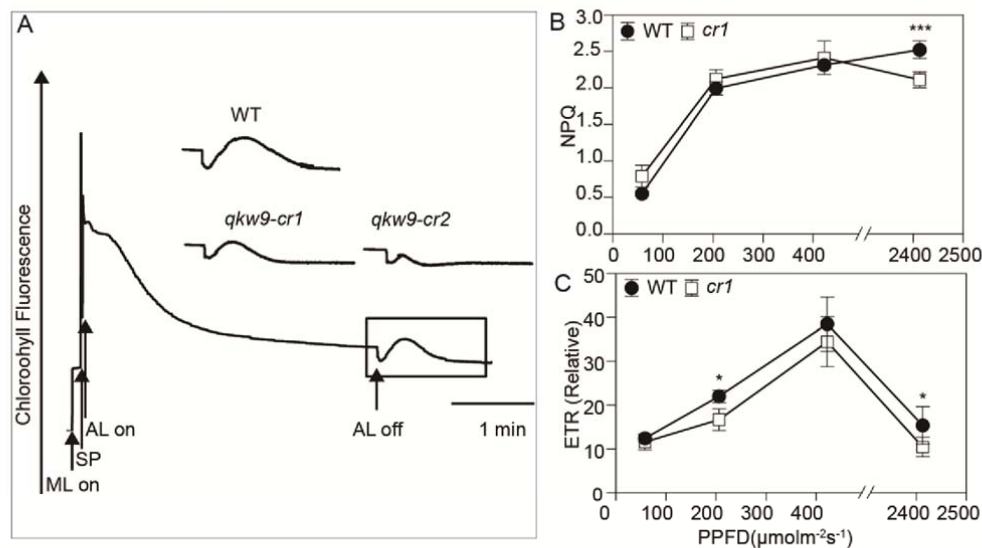
Figure 6. NDH activity monitoring and NPQ and ETR in null mutants of qKW9. (A) Monitoring of NDH activity using chlorophyll fluorescence analysis for *qkw9-cr1* and *qkw9-cr2* mutants. The curve shows the typical change trace of chlorophyll fluorescence *in vivo* as the NDH complex catalyzes the post-illumination reduction of the plastoquinone pool (Okuda et al., 2007). The change in post-illumination fluorescence ascribed to NDH activity was different between WT and mutants. Insets are magnified traces from the boxed area. ML, measuring light; AL, actinic light; SP, a saturating pulse of white light. **(B)** NPQ was induced by light intensity in both *cr*1 and WT, but it was significantly lower in *cr*1 under photon flux density of 2413 μmol of photons $m^{-2}s^{-1}$. **(C)** relative ETR (rETR) under different photon flux densities. rETR in cr1 and WT reached maximum when the light intensity was 422 μmol of photons $m^{-2}s^{-1}$. It was significantly lower in cr1 under the photon flux density of 206 μmol of photons $m^{-2}s^{-1}$ and 2413 μmol of photons $m^{-2}s^{-1}$. The rETR is depicted relative to a maximal value of ϕ_{PSII} × PPFD (photon flux density, μmol of photons $m^{-2}s^{-1}$). Data are shown as mean ± SD (*n*=6).

249   of 100 $\mu mols^{-2}m^{-1}$ in the field. These findings considerably differ from studies in Arabidopsis

250   and tobacco, since multiple mutant analyses have demonstrated that NDH does not function

251   to trigger thermal dissipation in PSII in these species (Burrows et al., 1998; Munekage et al.,

252   2004).

253   ***qKW9* controls kernel weight by regulating photosynthesis**

254   Genetic evidence suggests that physiological functions of cyclic electron transport (CET)

255   around Photosystem I (PSI) are essential for efficient photosynthesis and plant growth

256   (Munekage et al., 2004). The physiological role of CET is to protect PSII under intense light

257   via ΔpH-dependent thermal dissipation in PSII, as well as to act as an ATP generator in

258   photosynthesis (DalCorso et al., 2008; Alric and Johnson, 2017). Our results suggest that

259   reduced activity of the NDH complex in maize affected NPQ and ETR. We therefore asked

260   how photosynthesis and carbon assimilation were affected by changes in NDH activity? We

261   measured the fresh weight of developing kernels of NIL-SK and NIL-ZHENG58 under field

262   conditions, and investigated several photosynthesis-related parameters (Figure 7). Fresh

263   weight of NIL-SK kernels was similar to NIL-ZHENG58 before 30 DAP (Figure 7A).

264   However, kernels of NIL-SK reached their maximum fresh weight at 30DAP, while

265   NIL-ZHENG58 kernels continued to gain weight until 35 DAP, suggesting that carbon

266   deposition in kernels was greater in NIL-ZHENG58 at 35 DAP (Figure 7A). Consistent with

267   this observation, leaves of NIL-SK had more severe senescence at 30 DAP compared to

268   NIL-ZHENG58, indicating decreased source strength in the NIL-SK plants (Figure 1C).

269   NIL-SK also had significantly lower net photosynthesis than NIL-ZHENG58 at 22DAP and

270   30DAP (Figure 7B). Consistently, stomatal conductance and transpiration rate were similarly

271   lower in NIL-SK than in NIL-ZHENG58 (Figure 7C-7D). The lower photosynthetic capacity

272   of NIL-SK, coupled with the potential compensatory fact that less kernels were produced per

273   ear in this line (Table 1), may explain why the fresh weight of NIL-SK were not significantly

274   lower than NIL-ZHENG58 at 22DAP and 30DAP (Figure 7A). In addition, the chlorophyll

275   content (SPAD value) and the maximum photochemical efficiency (Fv/Fm) were invariant

276   between the NILs (Figure 7E-7F), indicating that the differences in the net photosynthetic

277   rates might not result from a different level of photosynthesis potential. Accordingly, the

278   photosynthetic rate was also significantly lower in *qKW9*-cr1 than WT at 30DAP under field

279   conditions (*qKW9*-cr1: 17.35±2.10 μmol $CO_2m^{-2}s^{-1}$, Wild type: 29.68±3.56μmol $CO_2\,m^{-2}s^{-1}$,

280   *n*=6). We conclude that impaired NDH activity affected both net photosynthesis and the
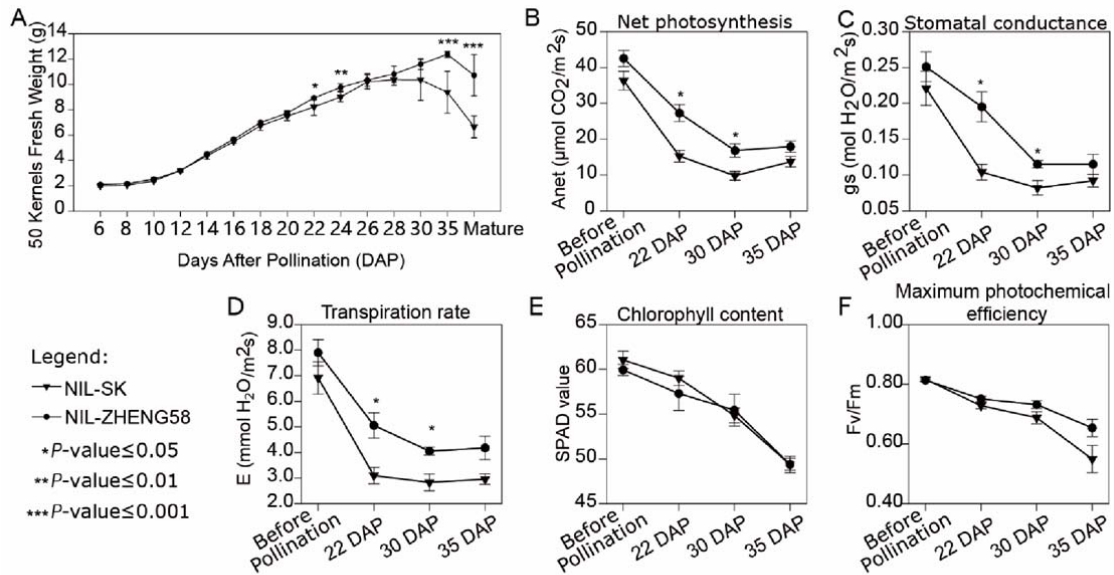
Figure 7. Grain filling and photosynthesis measurement in NIL-SK and NIL-Zheng58. **(A)** Time courses of fresh weight of 50 kernels of NIL-SK and NIL-Zheng58. The fresh weight of NIL-SK and NIL-ZHEGN58 reached the maximum at 30 DAP and 35 DAP, respectively. **(B)** to **(E)** Time courses of photosynthesis-rate related parameters of NIL-SK and NIL-Zheng58. Net photosynthesis **(B)**, stomatal conductance **(C)**, and transpiration rate **(D)** were significantly lower in NIL-SK than NIL-ZHENG58 at 22 DAP and 30 DAP; **(E)** chlorophyll content and **(F)** maximum photochemical efficiency did not show significant between genotype differences at any of the four stages tested. Data are shown as mean ± SD (*n*=6).

281   duration of active photosynthesis, resulting in smaller ears and kernels in NIL-SK.

282

DISCUSSION

***qKW9* encodes a PPR gene responsible for C-to-U editing of NdhB**

The maize kernel has been of interest to researchers as a model system for the study of development and genetics for a century. Numerous kernel mutants have been identified (Neuffer and Sheridan, 1980; Sheridan and Neuffer, 1980; Clark and Sheridan, 1991), and in recent years, many mutants that result in dramatically reduced kernel size, and seedling lethality have been identified. In many cases, *PPR* genes are responsible for these phenotypes, due to their function in organellar gene expression. Generally, null alleles of PPR genes in previous studies produce kernels that are with obvious development abnormality at early stages and are easily distinguished from normal kernels on self-crossed F_1 ears due to their smaller size, pale pericarp, flat or shrunken appearance (Manavski et al., 2012; Sosso et al., 2012; Li et al., 2014; Sun et al., 2015; Xiu et al., 2016; Cai et al., 2017; Chen et al., 2017; Qi et al., 2017; Ren et al., 2017; Dai et al., 2018; Li et al., 2018; Sun et al., 2019). Unlike these kernel mutants, kernels produced by null allele of *qKW9* are similar in appearance and viability although smaller in size comparing to wild type, and kernel weight is determined by genotype of maternal plant rather than kernel genotype. *qKW9* is the first identified C-to-U editing factor in the maize chloroplast that has a quantitative rather than qualitative effect on kernel and ear size. This difference stems from the involvement of *qKW9* in the abundance of the NDH complex, which in known to play a regulatory role in photosynthesis (Nashilevitz et al., 2010; Peltier et al., 2016). Based on results from this study, it is possible that variants of other yet-unidentified RNA editing factors responsible for the 11 C-to-U editing sites in maize *ndh* transcripts will also affect kernel and ear size in a quantitative way. Indeed, studies in *Arabidopsis* have identified many PPR genes affecting ndh expression, by focusing on changes in chlorophyll fluorescence related to NDH activity (Kotera et al., 2005; Okuda et al., 2007; Hammani et al., 2009; Okuda et al., 2010). Similar research in maize may help us rapidly identify potential QTL, circumventing the tedious work of fine mapping.

Grains are typical sink organs -i.e. they are net receivers of photoassimilates from photosynthetically active source tissues - and a considerable number of studies suggest that

311   enhancing photosynthetic efficiency could increase the productivity of crops (Sonnewald and

312   Fernie, 2018; South et al., 2019; Wu et al., 2019). In the light reactions of photosynthesis,

313   linear electron transport (LET) from water to $NADP^+$ does not fully satisfy the ATP/NADPH

314   production ratio required by the Calvin-Benson cycle and photorespiration (Yin and Struik,

315   2018). Cyclic electron transport (CET) around photosystem I (PSI) has, therefore, been

316   considered as a candidate for augmented ATP synthesis in response to fluctuating demand

317   during photosynthesis (Rumeau et al., 2007; DalCorso et al., 2008; Nakamura et al., 2013). In

318   PSI CET, electrons are recycled around PSI generating ΔpH and consequently ATP without a

319   concomitant accumulation of NADPH (Shikanai, 2007; Munekage and Taniguchi, 2016). In

320   Arabidopsis, two CET pathways have been identified by genetics. The main pathway depends

321   on PROTON GRADIENT REGULATION 5 (PGR5)/PGR5-LIKE PHOTOSYNTHETIC

322   PHENOTYPE 1 (PGRL1) proteins, whereas the minor pathway is mediated by the

323   chloroplast NADH dehydrogenase-like (NDH) complex (Munekage et al., 2004). The

324   Arabidopsis *pgr5* mutant is defective in PSI CET and was discovered by screening for

325   reduced non-photochemical quenching (NPQ) of chlorophyll fluorescence (Munekage et al.,

326   2002; DalCorso et al., 2008). However, as in tobacco, the Arabidopsis *chlororespiratory*

327   *reduction* (*crr*) mutants and *organelle transcript processing* (*otp*)mutants defective in

328   chloroplast NDH did not show any marked phenotype (Burrows et al., 1998; Hashimoto et al.,

329   2003; Munekage et al., 2004; Hammani et al., 2009; Okuda et al., 2010).

330   Plastid genomes encode 11 subunits (NdhA to NdhK) forming the core of the membrane

331   arm of the L-shaped structure of the NDH complex (Laughlin et al., 2019). Multiple PPR

332   genes regulate expression of *ndh* genes in Arabidopsis. These PPR genes are either

333   responsible for splicing of polycistronic transcripts, or site-specific C-to-U RNA editing

334   (Hashimoto et al., 2003; Munekage et al., 2004; Kotera et al., 2005; Okuda et al., 2007;

335   Hammani et al., 2009; Okuda et al., 2009; Okuda et al., 2010). C-to-U RNA editing is

336   important in organelle gene expression in various organisms, although the efficiency varies in

337   different organs and at different developmental stages (Maier et al., 1995; Peeters and Hanson,

338   2002). C-to-U RNA editing in Arabidopsis can generate translational initiation codons, as in

339   *CRR4* (Kotera et al., 2005) or cause amino acid alterations, as in *CRR21*, *CRR22*, *CRR28*,

340   *OTP82*, *OTP84* and *OTP85* (Okuda et al., 2007; Hammani et al., 2009; Okuda et al., 2009;

341   Okuda et al., 2010). Editing of *NdhB-246* in leaf tissues is near 100% in maize, suggesting that

342   it is important for the function of NdhB protein (Peeters and Hanson, 2002). *NdhB-246* editing

343   also occurs in tobacco and rice (Tsudzuki et al., 2001). Therefore, C-to-U editing of *NdhB-246*

344   appears crucial to its function. The *qKW9* QTL characterized in our study is the first RNA

345   editing factor that has been linked to C-to-U editing of *NdhB-246*. Our results clearly indicate

346   that the abolition of C-to-U editing in *NdhB-246* impairs accumulation of the NDH complex *in*

347   *vivo*.

348   **Cyclic electron transport via NDH complex in C$_4$ and C$_3$**

349   Chloroplast NDH mediation of CET around PSI was first reported in tobacco following

350   disruption of *NdhB* (Shikanai et al., 1998). Knockout lines of *ndh* genes were created by

351   plastid transformation in tobacco. Mutants defective in expression of chloroplast *ndh* genes

352   were isolated in Arabidopsis (Hashimoto et al., 2003). However, both knockout lines of *ndh*

353   genes in tobacco and mutants with impaired NDH activity in Arabidopsis lack morphological

354   phenotypes (Hashimoto et al., 2003; Munekage et al., 2004; Okuda et al., 2007; Hammani et

355   al., 2009; Okuda et al., 2009; Okuda et al., 2010). So, the general conclusion has been that

356   mutants defective in NDH do not show a clear phenotype and NDH is dispensable at least

357   when plants are grown in controlled environments. Analysis of this observation leads to the

358   conclusion that NDH does not function to generate a pH gradient in order to trigger thermal

359   dissipation in PSII. The observations we present here, where we found that *qKW9* is required

360   for the expression of *NdhB* and optimal activity of the NDH complex in maize, suggest that

361   this conclusion may not hold in all species. Namely in the null mutant genotypes, light

362   intensity-dependent ETR and NPQ were obviously affected. We additionally observed more

363   severe leaf senescence in NIL-SK, a phenonomon that may result from impaired thermal

364   dissipation, since NPQ induction under high-intensity light is suppressed as compared with

365   NIL-ZHENG58. Moreover, the overall rate of photosynthesis was also reduced in the null

366   *qKW9 mutant*, leading to significantly reduced ear and kernel size.

367   Our study of *qKW9* provides a possible explanation for the apparent contradiction of

368   these observations, in suggesting that CET via the NDH complex is more important in C_4

369   than in C_3 plants. CET around photosystem I is critical for balancing the photosynthetic

370   energy budget of the chloroplast by generating ATP without net production of NADPH

371   (Ishikawa et al., 2016a). C_4 plants have higher ATP requirements than C_3 plants (Ishikawa et

372   al., 2016b), rendering the ATP supply by CET particularly important, imply that during the

373   evolution of NADP-malic enzyme-type C_4 photosynthesis in the C_4-like genus *Flaveria*, CET

374   was promoted by markedly increasing expression of both PGR5/PGRL1 and NDH subunits

375   (Nakamura et al., 2013). The NDH subunit, however, increases markedly in bundle sheath

376   cells with the activity of the C_4 cycle while PGR5/PGRL1 increases in both mesophyll and

377   bundle sheath cells in *Flaveria* and other C_4 species, implying that the NDH complex

378   provides a considerable role in the establishment of C_4 photosynthesis (Nakamura et al.,

379   2013). Previously, it was also shown that NDH plays a central role in driving the

380   CO_2-concentrating mechanism in C_4 photosynthesis (Takabayashi et al., 2005; Andrews,

381   2010). In addition, the NDH complex has been experimentally demonstrated to be a

382   high-efficiency proton pump, increasing ATP production by cyclic electron transport (Strand

383   et al., 2017). Ishikawa et al. report that NDH-suppressed C_4 plants are characterized by

384   consistently decreased CO_2 assimilation rates, impaired proton translocation across the

385   thylakoid membrane and reduced growth rates (Ishikawa et al., 2016a). Results from our

386   study provide direct evidence that the NDH complex is important to C_4 photosynthesis. As

387   such comparison of our data with that from a recent study in Arabidopsis which showed that

388   NDH-dependent cyclic electron transport around PSI contributes to the generation of proton

389   motive force only in the weak mutant of *pgr5* (Nakano et al., 2019), suggests that it is more

390   important to C_4 than C_3 photosynthesis.

391   An alternative explanation could be the difference in the study conditions. In our study,

392   growth and photosynthesis measurement are conducted in the field where the plants

393   experience naturally fluctuating light, humidity, temperature, etc. Fluctuating elements may

394   give rise to stress to photosystems. Impairment of NDH-dependent PSI cyclic electron

395 transport causes a reduction in photosynthetic rate under fluctuating light, leading to

396 photoinhibition at PSI and consequently to reductions in plant biomass in rice (Yamori et al.,

397 2016). It is worth noting that there are studies stressing the role that NDH complex plays in

398 CET under stresses (Horváth et al., 2000; Wang et al., 2006; Yamori et al., 2015). Indeed the

399 conclusions that the NDH complexes role in CET is dispensable come from studies of tobacco

400 and Arabidopsis grown in growth chambers rather than the field, resulting in an

401 under-estimation of the importance of the NDH complex's regulatory effect on

402 photosynthesis.

403 In summary, our study identified a maize kernel size QTL which is caused by allelic

404 variation in *qKW9,* a PLS-DYW type PPR protein. We found that qKW9 is required for C-to-U

405 editing at 246th codon of *NdhB*, a chloroplast-encoded subunit of the NDH complex. With this

406 editing pattern previously being recorded occuring concomitantly with the onset of

407 photosynthetic activity in tobacco (Karcher and Bock, 2002). Functional characterization

408 revealed that C-to-U editing of maize *NdhB* is crucial for the accumulation of its protein

409 product as well as the activity of the NDH complex. This study thus challenges current models

410 of the role of the NDH in photosynthesis, revealing new insights into the regulation of C_4

411 photosynthesis and suggesting a novel potential target for crop improvement.

412 **METHODS AND MATERIALS**

413 **Fine mapping of *qKW9***

414 Multiple major QTL regulating kernel-size-related traits were identified by

415 multi-environment QTL analysis in ZHENG58×SK RIL population and a major QTL on

416 chromosome 9 regulating kernel width was designated as *qKW9* in a previous report (Raihan et

417 al., 2016). To fine-map *qKW9*, the heterogeneous inbred family (HIF) was screened against the

418 RIL population and RIL line KQ9-HZAU-1341-1 was heterozygous between Marker M2682

419 (155.83Mb in B73 Ref Gen v4) and Marker M3671 (156.83Mb in B73 RefGen v4) was used

420 as the founder HIF (Raihan et al., 2016). In a nursery grown in Hainan in 2015, two groups of

421 homozygous progenies of F1H5, which was a descendant of line KQ9-HZAU-1341-1, were

422 significantly different in hundred kernel weight (HKW), kernel length (KL), and kernel width

423   (KW). Thus, F1H5 was used as the starting HIF to fine map *qKW9* in this study. In the summer

424   of 2016, recombinants between Marker M2795 and Marker M3671 were screened against the

425   F1H5 population. In the winter of 2016, progeny tests were conducted on those recombinant

426   populations.

427   For genotyping, genomic DNA extraction from young leaf was conducted using the CTAB

428   protocol for plant tissues. To detect SNP and Indel markers, PCR was conducted in 10 μL

429   reactions with KASP master mix (cat no: KBS-1030-002, LGC), self-made KASP array mix,

430   and DNA template in 96 well non-transparent plates. KASP array mix was made by mixing

431   equal volumes of primer F1 (36 μM), F2 (36 μM), and R (90 μM) of a specific SNP marker. For

432   each reaction, 0.14 μL array mix, 1×master mix, and 20~200 ng DNA were used. Thermal

433   cycling was 94 ℃ for 15 minutes to activate the enzyme, followed by 10 cycles of touch down

434   PCR (denature at 94 ℃ for 20 s, annealing/elongation start with 61 ℃ for 60 s, drop 0.6 ℃ per

435   cycle), then annealing/elongation for another 26-36 cycles depending on the quality of primers

436   (denature at 94 ℃ for 20 s, annealing/elongation at 55 ℃ for 60 s). Upon the completion of the

437   KASP PCR, reaction plates were read by CFX96 Touch[TM] Real-time PCR detection system

438   and the data was then analysed with the Allelic Discrimination module of BioRad CFX

439   Manager 3.0. Detected signals were plotted against FAM and HEX fluorescence intensity as a

440   graph, with samples of the same genotype clustering together. To detect SSR markers, PCR

441   products were detected by AATI Fragment Analyzer following the manufacturer's instructions.

442   Maize plants were examined under natural field conditions in the experimental fields of

443   Wuhan (30°N, 114°E), Sanya (18°N, 109°E), and Baoding (39°N, 115°E) in China. The

444   planting density was 25 cm between adjacent plants in a row and the rows were 60 cm apart.

445   Field management, including irrigation, fertilizer application, and pest control, essentially

446   followed the normal agricultural practices. Harvested maize ears were air-dried and then

447   fully-developed ears were shelled for measuring HKW, KL, and KW as previously reported

448   (Raihan et al., 2016).

449   **BAC screen, sequence, and *de novo* assembly**

450   BACs covering *qKW9* of both parent lines-SK and ZHENG58- were screened. BAC DNA

22

451   was prepared using the QIAGEN Large-Construct Kit (Cat no: 12462) following the

452   manufacturer's instructions but with 150ml overnight-cultured bacterial input. The recovered

453   DNA was sent to a company (Nextomics Bioscience Co., Ltd, Wuhan, China) for quality

454   control and library construction. The resulting sequence data was assembled by PacBio's

455   open-source SMRT Analysis software.

456   **Fresh weight during the filling stage**

457   NILs derived from homozygous progenies of HIF-p11 were used to analyze the grain

458   filling rate of developing kernels after pollination. NILs with the *qKW9* allele of SK designated

459   as NIL-SK while NILs with the *qKW9* allele of ZHENG58 designated as NIL-ZHENG58.

460   Starting from 6 days after pollination (DAP), 50 fresh kernels were harvested and weighted

461   from 6 ears of each NIL every other day until 30 DAP. At 35 DAP and upon harvest fresh

462   kernels were also weighed.

463   **Mutagenesis of *qKW9* with CRISPR/Cas9-based gene editing**

464   Two guide RNA sequences (cggtggtggacatgtactg and ctgttctggggatccagct) against *qKW9*

465   were designed by CRISPR-P 2.0 (http://crispr.hzau.edu.cn/CRISPR2/) then cloned into a

466   CRISPR/Cas9 plant expression vector (Liu et al., 2017a). The backbone of the vector was

467   provided by WIMI Biotechnology Co., Ltd (Changzhou, China). The vector allows expression

468   of single guide RNA by the ZmU61 promoter and Cas9 by a maize UBI promoter. The

469   resulting binary plasmids were transformed into the Agrobacterium tumefaciens strain

470   EHA105 and used to transform maize inbred C01. All constructs were sequence-verified.

471   **Light Microscopy**

472   Whole sections of mature kernels were stained with iodine solution using the method in a

473   previous report (Zhao et al., 2016). Three different regions of endosperm were examined for

474   the morphology of starch.

475   **Subcellular localization of *qKW9***

476   *Zm00001d048451* was predicted to locate in chloroplast by TargetP (Emanuelsson et al.,

477   2007). To verify this, a codon-optimized CDS (optimized by a web tool -

478   https://www.genscript.com/codon_opt_pr.html) was fused with green fluorescent protein (GFP)

479   and driven by expression from the cauliflowner mosaic virus 35S promoter. The binary

480   vector-pK7FWG2.0-was obtained from Dr. Hannes Claeys (Cold Spring Harbor Laboratory,

481   USA). The plasmids containing the chimeric genes were transferred into Agrobacterium

482   tumefaciens strain GV3101. The resulting strain was co-infiltrated into *Nicotiana benthemiana*

483   leaves with a strain harboring P19 which was obtained from Dr. Edgar Demesa Arevalo (Cold

484   Spring Harbor Laboratory, USA) (Lindbo, 2007). Fluorescence signals were detected using

485   LSM780. DAPI (4,6-diamidino-2-phenylindole) staining solution

486   (http://cshprotocols.cshlp.org/content/2007/1/pdb.rec10850.full?text_only=true) was injected

487   to the leaf before observing the fluorescence signals. Agrobacterium growth and injection

488   followed the steps described in a previous report (Xu et al., 2015).

489   **Phylogenetic analysis**

490   To identify the PPR genes in maize B73 RefGen v4, protein sequences of B73 RefGen

491   v4 genes were downloaded from ftp://ftp.gramene.org/pub/gramene/ (B73 RefGen v4.59).

492   Then HMMER 3.0 software (Finn et al., 2011) was used to scan all of the annotated

493   Pentatricopeptide Repeat genes in B73 RefGen v4 with the Midden Markov (HMM) profile

494   of PPR domain (PF01535.20, http://pfam.sanger.ac.uk/) (E-value < 1). Based on the

495   C-terminal domain structure, the HMM profiles of E, E+, and DYW domain were rebuilt

496   using the previously predicted PPR genes in B73 RefGen v3. Then these HMM profiles were

497   used to scan the PPR genes annotated in B73 RefGen v4

498   (ftp://ftp.gramene.org/pub/gramene/CURRENT_RELEASE/gff3/zea_mays/gene_function).

499   Then TargetP version 1.1 (http://www.cbs.dtu.dk/services/TargetP/) was used to predict the

500   organelle targeting of these E, E+, and DYW types PPR proteins. Only the chloroplast

501   targeting genes were kept to conduct the evolutionary analysis with their orthologous genes

502   in Arabidopsis and rice

503   (https://download.maizegdb.org/Zm-B73-REFERENCE-GRAMENE-4.0/Orthologs/). The

504   evolutionary history was inferred using the Neighbor-Joining method (Saitou and Nei, 1987)

505   by MEGAX (Kumar et al., 2018). The bootstrap consensus tree inferred from 500 replicates

506   was taken to represent the evolutionary history of the taxa analyzed (Felsenstein, 1985).

24

507 **Photosynthetic parameters and chlorophyll content measurements**

508   Carbon dioxide assimilation rate, stomatal conductance, and transpiration rate were

509 measured on fully-expanded maize leaves grown in the field using a portable gas exchange

510 system (LI-6400XT, LI-COR Inc., USA) as described (Huang et al., 2009; Bihmidine et al.,

511 2013). The measurements were conducted at an ambient CO_2 concentration of 400 μmol

512 mol^{-1} and light saturation of 2000 μmol m^{-2} s^{-1}. Leaf photochemical efficiency (Fv/Fm) was

513 measured on dark-adapted leaves using the FlourPen FP100 chlorophyll fluorescence meter

514 (Photon System Instruments, Czech Republic). Leaf chlorophyll content was measured using

515 a chlorophyll meter (SPAD-502, Konica Minolta, Japan). The measurements were performed

516 before pollination and at 22, 30, and 35 days after pollination (DAP) on eight NIL-SK plants

517 or NIL-ZHENG58 plants. Means and standard errors (SE) were calculated using Microsoft

518 Excel. Differences in chlorophyll content and photosynthetic parameters were assessed using

519 the Student's *t*-test embedded in the Microsoft Excel program, at the *P*-value ≤ 0.05 level.

520 **RNA sequencing**

521   To explore the possible RNA editing in leaf by the PPR gene, the ear leaves from NIL-SK

522 and NIL-ZHENG58 plants before pollination and after pollination (22 days and 30 days) were

523 collected. Total RNA was isolated from these samples using Direct-zol RNA MiniPrep Plus kit

524 (Cat no: R2072, ZYMO Research, USA). Libraries were constructed using the Illumina

525 TruSeq Stranded RNA Kit (Illumina, San Diego, CA, USA) following the manufacturer's

526 recommendations. Strand-specific sequencing was performed on the Illumina HiSeq 2000

527 system (paired-end 100-bp reads). The raw reads were trimmed by Trimmomatic v0.36 (Bolger

528 et al., 2014) to gain high-quality clean reads, and the quality of the clean reads was checked

529 using the FASTQC program (Andrews, 2010). Next the clean reads were aligned to maize B73

530 RefGen v4 chloroplast genome by Hisat2 (Kim et al., 2015). Picard tools were subsequently

531 used   to   add   read   groups,   sort,   mark   duplicates,   and   create   index

532 (http://broadinstitute.github.io/picard/). Then the GATK was used to call the sequence variants

533 by HaplotypeCaller (McKenna et al., 2010). The ratio of edited allele reads count/total reads

25

534   count served as editing frequency for each site and the significance of editing frequency

535   difference between NIL-SK and NIL-ZHENG58 was estimated by pairwise *t*-test with a

536   threshold *P*-value < 0.05. Only the loci with a mean editing frequency difference over 5%

537   between NIL-SK and NIL-ZHENG58 were treated as possibly RNA editing sites being

538   affected by *qKW9*.

539   **RNA extraction and qRT-PCR**

540   Total RNA was extracted from various plant tissues except leaf using RNA extraction kit

541   (Cat no: 0416-50, Huayueyang, China). cDNA was synthesized from the extracted RNA using

542   the TransScript One-Step gDNA Removal and cDNA Synthesis SuperMix (Cat no: AT311,

543   TransGen Biotech, China). qRT-PCR was carried out in a total volume of 20 μl containing 2 μl

544   of 10x-diluted reverse-transcribed product, 0.2 mM gene-specific primers, and 10 μl KAPA

545   SYBR® FAST qPCR Master Mix (Cat no: KK4607), using a Bio-Rad CFX96 Touch^{TM}

546   Real-time PCR detection system according to the manufacturer's instructions. Quantitative

547   PCR was performed for the gene expression using QPIG, QPPR, and ACTIN primers (Table

548   S1).

549   **Immunoblot Analysis**

550   Chloroplast membrane proteins were isolated from the leaves of around 2-week-old

551   maize plants using kits (Cat no: BB-3175, BestBio, China). Protein samples were quantified

552   with BCA protein assay. The protein samples were separated by 12% SDS-PAGE. After

553   electrophoresis, the proteins were transferred onto a PVDF membrane (0.2 μm, Bio-Rad)

554   using Bio-Rad Semi-Dry Transfer Cell. The blot was blocked with 5% milk in TBST for 1h at

555   room temperature (RT) with agitation and then incubated in the primary antibody (from

556   Agrisera, AS16 4065) at a dilution of 1: 500 overnight in +4°C. The antibody solution was

557   decanted, and the blot was washed briefly with TBST at RT with agitation. The blot was

558   incubated in secondary antibody (anti-rabbit IgG horseradish peroxidase conjugated, from

559   Agrisera, AS09 602) diluted to 1:10 000 in 1% milk/TBST for 30min at RT with agitation.

560   The blot was washed briefly in TBST at RT with agitation and developed for 2 min with ECL

561   according to the manufacturer's instructions (Cat no: SL1350, Coolaber, China). The signals

562   were visualized by a GeneGnome chemiluminescence analyzer (Syngene).

563   **ASSESSION NUMBERS**

564   Sequence data from this article can be found in the GenBank/NCBI databases under the

565   SRA accession number: PRJNA588870.

566   **SUPPLEMENTARY DATA**

567   **Supplemental Figure S1** Schematic representation of genotypes and kernel weights of

568   recombinant families derived from F1H5.

569   **Supplemental Figure S2** qPCR analysis of Zm00001d048450 and Zm00001d048451

570   expression.

571   **Table S1** Primer sequences used in this study.

572   **ACKNOWLEDGEMENTS**

582   **FIGURE LEGENDS**

583   **Figure 1. Plant and kernel morphology of NIL-SK and NIL-Zheng58. (A)** NIL-SK (NS)

584   and NIL-Zheng58 (NZ) had very similar plant architecture, Bar=20cm. **(B)** NIL-SK (NS)

585   two-week old seedlings were smaller than NIL-Zheng58 (NZ). Bar=4cm. **(C)** Leaf senescence

586   was greater in NIL-SK (NS) at 30 days after pollination compared to NIL-Zheng58. Bar=10cm.

587   **(D)** Ears of NIL-SK (NS) were smaller than in NIL-Zheng58 (NZ). Bar=1cm. **(E) to (J)**

588   Mature kernels of NIL-SK (E-G) were smaller that in NIL-Zheng58 (H-J).   Whole kernels of

589   NIL-SK and NIL-Zheng58 (**[E]** and **[H]**). Bar=2mm; transverse section of kernel of NIL-SK

590   and NIL-Zheng58(**[F]** and **[I]**). Bar=2mm; Longitudinal section of kernel of NIL-SK and

591   NIL-Zheng58(**[G]** and **[J]**). Bar=2mm; **(K) to (R)** Similar starch structure in endosperms of

592   mature kernels of NIL-SK and NIL-Zheng58. Whole longitudinal section stained with iodine

593   solution of kernels of NIL-SK and NIL-Zheng58 (**[K]** and **[O]**), 1, 2, 3 indicate the crown,

594   farinaceous and keratin endosperm regions, respectively. Bar=1mm; **(L) to (N)** correspond to

595   regions 1, 2, 3 in **(K)**; and **(P) to (R)** correspond to regions 1, 2, 3 in **(O)**. Bar=10μm.

596

597   **Figure 2. Fine mapping and gene structure of *qKW9*. (A)** Mapping delimits *qKW9* to the

598   region between M3484 and M3506 on chromosome 9. F1H5 which derives from ZHENG58 ×

599   SK RIL population is the founder line for screening heterozygous inbred families (HIFs) for

600   fine mapping *qKW9*. Progeny tests of kernel weight were conducted on the resulting

601   recombinant families. White bar represents the homozygous chromosomal segment for SK,

602   grey bar represents the heterozygous chromosomal segment for ZHENG58 × SK, black bar

603   represents the homozygous chromosomal segment for ZHENG58. The graphical genotype

604   represents F1H5. Numbers between markers represent physical distances (Kb) between the

605   adjacent markers and numbers in brackets represent the number of recombinants. **(B)** Gene

606   annotations in the region of *qKW9* of B73, SK, and Zheng58. Sequences were obtained by

607   sequencing BACs covering *qKW9* from SK and ZHENG58 genome BAC libraries,

608   respectively. Zm00001d048452 was absent in both SK and ZHENG58. Two candidate

609   genes-*Zm00001d048450* and *Zm00001d048451*- were identified in *qKW9*. **(C)**

610   *Zm00001d048451* is a 1.8kb intron-less gene with 8 pentatricopeptide repeats and a

611   13bp-deletion was identified in coding region of *Zm00001d048451* in SK. CRISPR/Cas9 was

612   used to create knockout mutants with a single guide sequence (the 20bp sequence adjacent to

613   PAM) targeting *Zm00001d048451* in the inbred C01. Two mutated alleles - *qkw9-cr1* and

614   *qkw9-cr2* - were identified by sequencing the first-generation (T_0) plants and used for further

615   genetic analysis.

28

616

617   **Figure 3. Two CRISPR/Cas9 knockout mutants of Zm00001d048451-*qkw9-cr1* and**

618   ***qkw9-cr2*-produced smaller ears and smaller kernels than wild type.** Each mutant is shown

619   alongside its corresponding wild type segregant from a single Cas9-free T_1 generation plant. **(A)**

620   and **(B)** comparison of ears produced by CRISPR/Cas9 mutants (left) and WT (right).

621   *qkw9-cr1* (left) and wild type (right) in **(A)** and *qkw9-cr2* (left) and wild type (right) in **(B)**.

622   Bar=1cm. **(D)** and **(E)** kernels produced by CRISPR/Cas9 mutants (lower row) were smaller

623   than WT (upper row). *qkw9-cr1* (lower) and wild type (upper) in **(D)** and *qkw9-cr2* (lower)

624   and wild type (upper) in **(E)**. Bar=1cm. **(C)** and **(F)** show reductions in ear weight **(C)** and

625   kernel weight **(F)** of CRISPR/Cas9 knockout mutants. Data are shown as mean ± SD (n=6).

626   *** P < 0.001.

627

628   **Figure 4. Characterization of *qKW9/Zm00001d048451*. (A)** Phylogenetic tree of maize,

629   Arabidopsis and rice PLS-E, PLE-E+, and PLS-DYW Pentatricopeptide Repeat genes

630   predicted to localize in chloroplast/plastid by TargetP . **(B)** Autofluorescence of chlorophyll

631   (red). **(C)** qKW9-GFP fusion protein (green) in green puncta within plastids **(D)** DAPI

632   staining (blue) of nuclei **(E)** Overlay of **(B), (C)** and **(D)**. Scale bar=5 μm. **(F)** Allele in

633   NIL-SK of *Zm00001d048451* fails to edit C to U in 246th codon of *NdhB* gene. C-to-U editing

634   in NdhB-246 results in amino acid change from proline to leucine. Pro, proline; Leu, leucine.

635

636   **Figure 5. Protein blot analysis of the NDH complex.** Chloroplast membrane protein was

637   extracted with a commercial kit and protein samples were quantified with BCA protein assay.

638   1× sample amount equals 40 μg protein. Antibody against NdhH was used to indicate the

639   amout of NDH complex. Chloroplast membrane protein from NIL-ZHENG58 was loaded a

640   series of dilutions as indicated. Specific bands corresponded in size of NdhH protein

641   (expected in 45 kDa, apparent in 49 kDa). Signals in NIL-ZHENG58 declined along with the

642   dilution. The level of NdhH in NIL-SK was reduced to less than 25% of NIL-ZHENG58.

643   Coomassie R-250 staining was used to show the proteins separated by electropheris as a

644   loading control.

645

646   **Figure 6**. **NDH activity monitoring and NPQ and ETR in null mutants of qKW9. (A)**
647   Monitoring of NDH activity using chlorophyll fluorescence analysis for *qkw9-cr1* and
648   *qkw9-cr2* mutants. The curve shows the typical change trace of chlorophyll fluorescence *in*
649   *vivo* as the NDH complex catalyzes the post-illumination reduction of the plastoquinone pool
650   (Okuda et al., 2007). The change in post-illumination fluorescence ascribed to NDH activity
651   was different between WT and mutants. Insets are magnified traces from the boxed area. ML,
652   measuring light; AL, actinic light; SP, a saturating pulse of white light. **(B)** NPQ was induced
653   by light intensity in both *cr*1 and WT, but it was significantly lower in *cr*1 under photon flux
654   density of 2413 μmol of photons $m^{-2}s^{-1}$. **(C)** relative ETR (rETR) under different photon flux
655   densities. rETR in cr1 and WT reached maximum when the light intensity was 422 μmol of
656   photons $m^{-2}s^{-1}$. It was significantly lower in *cr*1 under the photon flux density of 206 μmol of
657   photons $m^{-2}s^{-1}$ and 2413 μmol of photons $m^{-2}s^{-1}$. The rETR is depicted relative to a maximal
658   value of ϕ_{PSII} × PPFD (photon flux density, μmol of photons $m^{-2}s^{-1}$). Data are shown as mean ±
659   SD (*n*=6).

660

661   **Figure 7**. **Grain filling and photosynthesis measurement in NIL-SK and NIL-Zheng58.**
662   **(A)** Time courses of fresh weight of 50 kernels of NIL-SK and NIL-Zheng58. The fresh weight
663   of NIL-SK and NIL-ZHEGN58 reached the maximum at 30 DAP and 35 DAP, respectively. **(B)**
664   to **(E)** Time courses of photosynthesis-rate related parameters of NIL-SK and NIL-Zheng58.
665   Net photosynthesis **(B)**, stomatal conductance (C), and transpiration rate **(D)** were significantly
666   lower in NIL-SK than NIL-ZHENG58 at 22 DAP and 30 DAP; **(E)** chlorophyll content and **(F)**
667   maximum photochemical efficiency did not show significant between genotype differences at
668   any of the four stages tested. Data are shown as mean ± SD (*n*=6).

669

670

671 **Table 1.** Ear related and agronomic traits in NIL-SK and NIL-Zheng58.

Trait	NIL-SK		NIL-Zheng58		P-value
	Mean ± SD[a]	N[b]	Mean ± SD	N	
Hundred Kernel Weight/g	15.59 ± 2.01	27	18.57±1.21	30	6.07×10^{-9}
Ear Length/cm	9.75 ± 0.75	31	10.68±0.76	37	3.72×10^{-6}
Kernel Number per Row	22.00±2.99	27	24.03±2.28	32	4.47×10^{-3}
Ear Row Number	12.43±1.00	28	12.39±0.80	36	0.86
Kernel Number per Ear	249.22±39.45	27	279.39±34.28	31	2.89×10^{-3}
Ear Weight/g	43.79±7.60	30	57.33±8.35	36	3.74×10^{-9}
Kernel Weight per Ear/g	38.84±6.60	19	53.68±7.44	17	3.07×10^{-7}
Plant Height/cm	190.73±10.52	92	195.29±10.12	91	3.22×10^{-3}
Ear Height/cm	84.48±7.19	92	83.65±9.68	91	0.51
Days to Shedding/Day	63.38±1.81	68	60.16±1.21	70	6.72×10^{-24}

672 [a] SD=standard deviation; [b]N, number of observed individuals.

673

674

675   **Table 2** C-to-U editing sites in plastid genes with significant editing frequency difference

676   between NIL-SK and NIL-Zheng58.

Locus(transcript)	Genome position	Feature	Developing Stages	Editing level%		P-value	Editing difference %
				NIL-SK	NIL-Zheng58		
GRMZM5G876106(NdhB)	90736	CDS, P>L	Before Pollination	0.00	100.00	NA	100.00
			22 DAP[a]	0.00	100.00		
			30 DAP	0.00	100.00		
GRMZM5G810298 (NdhB)	132001	CDS, P>L	Before Pollination	0.00	97.05	2.00E-05	98.15
			22 DAP	0.00	98.79		
			30 DAP	0.00	98.60		
intergenic	65407		Before Pollination	0.00	72.73	0.0041	87.21
			22 DAP	0.00	88.89		
			30 DAP	0.00	100.00		
GRMZM5G866064	139970	CDS, synonymous	Before Pollination	26.64	36.36	0.024	8.96
			22 DAP	18.52	30.60		
			30 DAP	27.87	32.95		
GRMZM5G856777	8558	5'UTR	Before Pollination	9.40	16.77	0.044	5.82
			22 DAP	31.63	39.61		
			30 DAP	35.50	37.63		
GRMZM5G845244 (rps8)	78717	CDS, S>L	Before Pollination	89.36	96.92	0.048	5.79
			22 DAP	98.08	100.00		
			30 DAP	92.11	100.00		

677   [a] DAP= days after pollination.

678

679

680

681

Parsed Citations

Alric J, Johnson X (2017) Alternative electron transport pathways in photosynthesis: a confluence of regulation. Curr Opin Plant Biol 37: 78–86

Pubmed: Author and Title
Google Scholar: Author Only Title Only Author and Title

Andrews S (2010) FastQC: a quality control tool for high throughput sequence data.

Barkan A, Small I (2014) Pentatricopeptide Repeat Proteins in Plants. Annu Rev Plant Biol 65: 415–442

Pubmed: Author and Title
Google Scholar: Author Only Title Only Author and Title

Bihmidine S, Hunter CT, Johns CE, Koch KE, Braun DM (2013) Regulation of assimilate import into sink organs: Update on molecular drivers of sink strength. Front Plant Sci. doi: 10.3389/fpls.2013.00177

Pubmed: Author and Title
Google Scholar: Author Only Title Only Author and Title

Bolger AM, Lohse M, Usadel B (2014) Trimmomatic: A flexible trimmer for Illumina sequence data. Bioinformatics 30: 2114–2120

Pubmed: Author and Title
Google Scholar: Author Only Title Only Author and Title

Burrows PA, Sazanov LA, Svab Z, Maliga P, Nixon PJ (1998) Identification of a functional respiratory complex in chloroplasts through analysis of tobacco mutants containing disrupted plastid ndh genes. EMBO J 17: 868–876

Pubmed: Author and Title
Google Scholar: Author Only Title Only Author and Title

Cai M, Li S, Sun F, Sun Q, Zhao H, Ren X, Zhao Y, Tan BC, Zhang Z, Qiu F (2017) Emp10 encodes a mitochondrial PPR protein that affects the cis-splicing of nad2 intron 1 and seed development in maize. Plant J 91: 132–144

Pubmed: Author and Title
Google Scholar: Author Only Title Only Author and Title

Chateigner-Boutin AL, Small I (2010) Plant RNA editing. RNA Biol 7: 213–219

Pubmed: Author and Title
Google Scholar: Author Only Title Only Author and Title

Chen X, Feng F, Qi W, Xu L, Yao D, Wang Q, Song R (2017) Dek35 Encodes a PPR Protein that Affects cis-Splicing of Mitochondrial nad4 Intron 1 and Seed Development in Maize. Mol Plant 10: 427–441

Pubmed: Author and Title
Google Scholar: Author Only Title Only Author and Title

Clark JK, Sheridan F (1991) Isolation and Characterization of 51 embryo-specific Mutations of Maize. Plant Cell 3: 935–951

Pubmed: Author and Title
Google Scholar: Author Only Title Only Author and Title

Dai D, Luan S, Chen X, Wang Q, Feng Y, Zhu C, Qi W, Song R (2018) Maize Dek37 encodes a P-type PPR protein that affects cis-splicing of mitochondrial nad2 intron 1 and seed development. Genetics 208: 1069–1082

Pubmed: Author and Title
Google Scholar: Author Only Title Only Author and Title

DalCorso G, Pesaresi P, Masiero S, Aseeva E, Schünemann D, Finazzi G, Joliot P, Barbato R, Leister D (2008) A Complex Containing PGRL1 and PGR5 Is Involved in the Switch between Linear and Cyclic Electron Flow in Arabidopsis. Cell 132: 273–285

Pubmed: Author and Title
Google Scholar: Author Only Title Only Author and Title

Emanuelsson O, Brunak S, von Heijne G, Nielsen H (2007) Locating proteins in the cell using TargetP, SignalP and related tools. Nat Protoc 2: 953–971

Pubmed: Author and Title
Google Scholar: Author Only Title Only Author and Title

Felsenstein J (1985) Confidence Limits on Phylogenies: An Approach Using the Bootstrap. Evolution (N Y) 39: 783

Pubmed: Author and Title
Google Scholar: Author Only Title Only Author and Title

Finn RD, Clements J, Eddy SR (2011) HMMER web server: Interactive sequence similarity searching. Nucleic Acids Res. doi: 10.1093/nar/gkr367

Pubmed: Author and Title
Google Scholar: Author Only Title Only Author and Title

Hammani K, Okuda K, Tanz SK, Chateigner-Boutin A-L, Shikanai T, Small I (2009) A Study of New Arabidopsis Chloroplast RNA Editing Mutants Reveals General Features of Editing Factors and Their Target Sites. Plant Cell 21: 3686–3699

Pubmed: Author and Title
Google Scholar: Author Only Title Only Author and Title

Hashimoto M, Endo T, Peltier G, Tasaka M, Shikanai T, Wise RP, Pring DR (2003) A nucleus-encoded factor, CRR2, is essential for the expression of chloroplast ndhB in Arabidopsis. Plant J 36: 541–549

Pubmed: Author and Title
Google Scholar: Author Only Title Only Author and Title

Horváth EM, Peter SO, Joët T, Rumeau D, Cournac L, Horváth G V., Kavanagh TA, Schäfer C, Peltier G, Medgyesy P (2000) Targeted Inactivation of the Plastid ndhB Gene in Tobacco Results in an Enhanced Sensitivity of Photosynthesis to Moderate Stomatal Closure. Plant Physiol 123: 1337–1350

Pubmed: Author and Title
Google Scholar: Author Only Title Only Author and Title

Huang M, Slewinski TL, Baker RF, Janick-Buckner D, Buckner B, Johal GS, Braun DM (2009) Camouflage patterning in maize leaves results from a defect in porphobilinogen deaminase. Mol Plant 2: 773–789

Pubmed: Author and Title
Google Scholar: Author Only Title Only Author and Title

Ishikawa N, Takabayashi A, Noguchi K, Tazoe Y, Yamamoto H, Von Caemmerer S, Sato F, Endo T (2016a) NDH-mediated cyclic electron flow around photosystem I is crucial for C4 photosynthesis. Plant Cell Physiol 57: 2020–2028

Pubmed: Author and Title
Google Scholar: Author Only Title Only Author and Title

Ishikawa N, Takabayashi A, Sato F, Endo T (2016b) Accumulation of the components of cyclic electron flow around photosystem I in C4 plants, with respect to the requirements for ATP. Photosynth Res 129: 261–277

Pubmed: Author and Title
Google Scholar: Author Only Title Only Author and Title

Karcher D, Bock R (2002) The amino acid sequence of a plastid protein is developmentally regulated by RNA editing. J Biol Chem 277: 5570–5574

Pubmed: Author and Title
Google Scholar: Author Only Title Only Author and Title

Kim D, Langmead B, Salzberg SL (2015) HISAT: A fast spliced aligner with low memory requirements. Nat Methods 12: 357–360

Pubmed: Author and Title
Google Scholar: Author Only Title Only Author and Title

Kotera E, Tasaka M, Shikanai T (2005) A pentatricopeptide repeat protein is essential for RNA editing in chloroplasts. Nature 433: 326–330

Pubmed: Author and Title
Google Scholar: Author Only Title Only Author and Title

Kumar S, Stecher G, Li M, Knyaz C, Tamura K (2018) MEGA X: Molecular evolutionary genetics analysis across computing platforms. Mol Biol Evol 35: 1547–1549

Pubmed: Author and Title
Google Scholar: Author Only Title Only Author and Title

Laughlin TG, Bayne AN, Trempe J-F, Savage DF, Davies KM (2019) Structure of the complex I-like molecule NDH of oxygenic photosynthesis. Nature 566: 411–414

Pubmed: Author and Title
Google Scholar: Author Only Title Only Author and Title

Li Q, Li L, Yang X, Warburton ML, Bai G, Dai J, Li J, Yan J (2010a) Relationship, evolutionary fate and function of two maize co-orthologs of rice GW2 associated with kernel size and weight. BMC Plant Biol 10: 143

Pubmed: Author and Title
Google Scholar: Author Only Title Only Author and Title

Li Q, Yang X, Bai G, Warburton ML, Mahuku G, Gore M, Dai J, Li J, Yan J (2010b) Cloning and characterization of a putative GS3 ortholog involved in maize kernel development. Theor Appl Genet 120: 753–763

Pubmed: Author and Title
Google Scholar: Author Only Title Only Author and Title

Li X, Gu W, Sun S, Chen Z, Chen J, Song W, Zhao H, Lai J (2018) Defective Kernel 39 encodes a PPR protein required for seed development in maize. J Integr Plant Biol 60: 45–64

Pubmed: Author and Title
Google Scholar: Author Only Title Only Author and Title

Li XJ, Zhang YF, Hou M, Sun F, Shen Y, Xiu ZH, Wang X, Chen ZL, Sun SSM, Small I, et al (2014) Small kernel 1 encodes a pentatricopeptide repeat protein required for mitochondrial nad7 transcript editing and seed development in maize (Zea mays) and rice (Oryza sativa). Plant J 79: 797–809

Pubmed: Author and Title
Google Scholar: Author Only Title Only Author and Title

Lindbo JA (2007) High-efficiency protein expression in plants from agroinfection-compatible Tobacco mosaic virus expression vectors. BMC Biotechnol 7: 1–11

Pubmed: Author and Title
Google Scholar: Author Only Title Only Author and Title

Liu H, Ding Y, Zhou Y, Jin W, Xie K, Chen LL (2017a) CRISPR-P 2.0: An Improved CRISPR-Cas9 Tool for Genome Editing in Plants. Mol Plant 10: 530–532

Pubmed: Author and Title
Google Scholar: Author Only Title Only Author and Title

Liu J, Deng M, Guo H, Raihan S, Luo J, Xu Y, Dong X, Yan J (2015) Maize orthologs of rice GS5 and their trans-regulator are associated with kernel development. J Integr Plant Biol 57: 943–953

Pubmed: Author and Title
Google Scholar: Author Only Title Only Author and Title

Liu J, Huang J, Guo H, Lan L, Wang H, Xu Y, Yang X, Li W, Tong H, Xiao Y, et al (2017b) The conserved and unique genetic architecture of kernel size and weight in maize and rice. Plant Physiol 175: 774–785

Pubmed: Author and Title
Google Scholar: Author Only Title Only Author and Title

Liu N, Liu J, Li W, Pan Q, Liu J, Yang X, Yan J, Xiao Y (2018) Intraspecific variation of residual heterozygosity and its utility for quantitative genetic studies in maize. BMC Plant Biol 18: 66

Pubmed: Author and Title
Google Scholar: Author Only Title Only Author and Title

Lurin C, Andres C, Aubourg S, Bellaoui M, Bitton F, Bruyere C, Caboche M, Debast C, Gualberto J, Hoffmann H, et al (2004) Genome-wide Analysis of Arabidopsis Pentatricopeptide Repeat Proteins Reveals Their Essential Role in Organelle Biogenesis. Plant Cell 16: 2089–2103

Pubmed: Author and Title
Google Scholar: Author Only Title Only Author and Title

Maier RM, Neckermann K, Igloi GL, Koössel H (1995) Complete sequence of the maize chloroplast genome: Gene content, hotspots of divergence and fine tuning of genetic information by transcript editing. J Mol Biol 251: 614–628

Pubmed: Author and Title
Google Scholar: Author Only Title Only Author and Title

Manavski N, Guyon V, Meurer J, Wienand U, Brettschneider R (2012) An Essential Pentatricopeptide Repeat Protein Facilitates 5' Maturation and Translation Initiation of rps3 mRNA in Maize Mitochondria. Plant Cell 24: 3087–3105

Pubmed: Author and Title
Google Scholar: Author Only Title Only Author and Title

McCarty DR (2017) Maize kernel development. In B Larkins, ed, Maize kernel Dev. CABI, pp 44–55

Pubmed: Author and Title
Google Scholar: Author Only Title Only Author and Title

McKenna A, Hanna M, Banks E, Sivachenko A, Cibulskis K, Kernytsky A, Garimella K, Altshuler D, Gabriel S, Daly M, et al (2010) The genome analysis toolkit: A MapReduce framework for analyzing next-generation DNA sequencing data. Genome Res 20: 1297–1303

Pubmed: Author and Title
Google Scholar: Author Only Title Only Author and Title

Munekage Y, Hashimoto M, Miyake C, Tomizawa KI, Endo T, Tasaka M, Shikanai T (2004) Cyclic electron flow around photosystem I is essential for photosynthesis. Nature 429: 579–582

Pubmed: Author and Title
Google Scholar: Author Only Title Only Author and Title

Munekage Y, Hojo M, Meurer J, Endo T, Tasaka M, Shikanai T (2002) PGR5 is involved in cyclic electron flow around photosystem I and is essential for photoprotection in Arabidopsis. Cell 110: 361–371

Pubmed: Author and Title
Google Scholar: Author Only Title Only Author and Title

Munekage YN, Taniguchi YY (2016) Promotion of Cyclic Electron Transport Around Photosystem I with the Development of C4 Photosynthesis. Plant Cell Physiol 57: 897–903

Pubmed: Author and Title
Google Scholar: Author Only Title Only Author and Title

Nakamura N, Iwano M, Havaux M, Yokota A, Munekage YN (2013) Promotion of cyclic electron transport around photosystem I during the evolution of NADP-malic enzyme-type C4 photosynthesis in the genus Flaveria. New Phytol 199: 832–842

Pubmed: Author and Title
Google Scholar: Author Only Title Only Author and Title

Nakano H, Yamamoto H, Shikanai T (2019) contribution of NDH-dependent cyclic electron transport around photosyst. BBA-Bioenergetics 1860: 369–374

Pubmed: Author and Title
Google Scholar: Author Only Title Only Author and Title

Nashilevitz S, Melamed-Bessudo C, Izkovich Y, Rogachev I, Osorio S, Itkin M, Adato A, Pankratov I, Hirschberg J, Fernie AR, et al (2010) An orange ripening mutant links plastid NAD(P)H dehydrogenase complex activity to central and specialized metabolism during tomato fruit maturation. Plant Cell 22: 1977–1997

Pubmed: Author and Title
Google Scholar: Author Only Title Only Author and Title

Neuffer MG, Sheridan WF (1980) DEFECTIVE KERNEL MUTANTS OF MAIZE . I . GENETIC AND LETHALITY STUDIES. Genetics 95: 929–944

Pubmed: Author and Title
Google Scholar: Author Only Title Only Author and Title

Okuda K, Chateigner-Boutin A-L, Nakamura T, Delannoy E, Sugita M, Myouga F, Motohashi R, Shinozaki K, Small I, Shikanai T (2009) Pentatricopeptide Repeat Proteins with the DYW Motif Have Distinct Molecular Functions in RNA Editing and RNA Cleavage in Arabidopsis Chloroplasts . Plant Cell 21: 146–156

Pubmed: Author and Title
Google Scholar: Author Only Title Only Author and Title

Okuda K, Hammani K, Tanz SK, Peng L, Fukao Y, Myouga F, Motohashi R, Shinozaki K, Small I, Shikanai T (2010) The pentatricopeptide repeat protein OTP82 is required for RNA editing of plastid ndhB and ndhG transcripts. Plant J 61: 339–349

Pubmed: Author and Title
Google Scholar: Author Only Title Only Author and Title

Okuda K, Myouga F, Motohashi R, Shinozaki K, Shikanai T (2007) Conserved domain structure of pentatricopeptide repeat proteins involved in chloroplast RNA editing. Proc Natl Acad Sci 104: 8178–8183

Pubmed: Author and Title
Google Scholar: Author Only Title Only Author and Title

Peeters NM, Hanson MR (2002) Transcript abundance supercedes editing efficiency as a factor in developmental variation of chloroplast gene expression. RNA 8: 497–511

Pubmed: Author and Title
Google Scholar: Author Only Title Only Author and Title

Peltier G, Aro E, Shikanai T (2016) NDH-1 and NDH-2 Plastoquinone Reductases in Oxygenic Photosynthesis. Annu Rev Plant Biol 67: 55–80

Pubmed: Author and Title
Google Scholar: Author Only Title Only Author and Title

Qi W, Tian Z, Lu L, Chen X, Chen X, Zhang W, Song R (2017) Editing of mitochondrial transcripts nad3 and cox2 by dek10 is essential for mitochondrial function and maize plant development. Genetics 205: 1489–1501

Pubmed: Author and Title
Google Scholar: Author Only Title Only Author and Title

Raihan MS, Liu J, Huang J, Guo H, Pan Q, Yan J (2016) Multi-environment QTL analysis of grain morphology traits and fine mapping of a kernel-width QTL in Zheng58 × SK maize population. Theor Appl Genet 129: 1465–1477

Pubmed: Author and Title
Google Scholar: Author Only Title Only Author and Title

Ren X, Pan Z, Zhao H, Zhao J, Cai M, Li J, Zhang Z, Qiu F, Leubner G (2017) EMPTY PERICARP11 serves as a factor for splicing of mitochondrial nad1 intron and is required to ensure proper seed development in maize. J Exp Bot 68: 4571–4581

Pubmed: Author and Title
Google Scholar: Author Only Title Only Author and Title

Rumeau D, Peltier G, Cournac L (2007) Chlororespiration and cyclic electron flow around PSI during photosynthesis and plant stress response. Plant, Cell Environ 30: 1041–1051

Pubmed: Author and Title
Google Scholar: Author Only Title Only Author and Title

Ruwe H, Castandet B, Schmitz-Linneweber C, Stern DB (2013) Arabidopsis chloroplast quantitative editotype. FEBS Lett 587: 1429–1433

Pubmed: Author and Title
Google Scholar: Author Only Title Only Author and Title

Ruwe H, Gutmann B, Schmitz-Linneweber C, Small I, Kindgren P (2019) The E domain of CRR2 participates in sequence-specific recognition of RNA in plastids. New Phytol 222: 218–229

Pubmed: Author and Title
Google Scholar: Author Only Title Only Author and Title

Saitou N, Nei M (1987) The neighbor-joining method: a new method for reconstructing phylogenetic trees. Mol Biol Evol 4: 406–425

Pubmed: Author and Title
Google Scholar: Author Only Title Only Author and Title

Scanlon MJ, Takacs EM (2009) Kernel biology. In J Bennetzen, S Hake, eds, Handb. Maize Its Biol. Springer, New York, NY, pp 121–143

Pubmed: Author and Title
Google Scholar: Author Only Title Only Author and Title

Schmitz-Linneweber C, Small I (2008) Pentatricopeptide repeat proteins: a socket set for organelle gene expression. Trends Plant Sci 13: 663–670

Pubmed: Author and Title

Google Scholar: Author Only Title Only Author and Title

Sheridan WF, Neuffer MG (1980) Defective kernel mutants of maize II. morphological and embryo culture studies. Genetics 95: 945–960
Pubmed: Author and Title
Google Scholar: Author Only Title Only Author and Title

Shikanai T (2007) Cyclic Electron Transport Around Photosystem I: Genetic Approaches. Annu Rev Plant Biol 58: 199–217
Pubmed: Author and Title
Google Scholar: Author Only Title Only Author and Title

Shikanai T, Endo T, Hashimoto T, Yamada Y, Asada K, Yokota A (1998) Directed disruption of the tobacco ndhB gene impairs cyclic electron flow around photosystem I. Proc Natl Acad Sci 95: 9705–9709
Pubmed: Author and Title
Google Scholar: Author Only Title Only Author and Title

Sonnewald U, Fernie AR (2018) Next-generation strategies for understanding and influencing source–sink relations in crop plants. Curr Opin Plant Biol 43: 63–70
Pubmed: Author and Title
Google Scholar: Author Only Title Only Author and Title

Sosso D, Luo D, Li Q-B, Sasse J, Yang J, Gendrot G, Suzuki M, Koch KE, McCarty DR, Chourey PS, et al (2015) Seed filling in domesticated maize and rice depends on SWEET-mediated hexose transport. Nat Genet 47: 1489–1493
Pubmed: Author and Title
Google Scholar: Author Only Title Only Author and Title

Sosso D, Mbelo S, Vernoud V, Gendrot G, Dedieu A, Chambrier P, Dauzat M, Heurtevin L, Guyon V, Takenaka M, et al (2012) PPR2263, a DYW-Subgroup Pentatricopeptide Repeat Protein, Is Required for Mitochondrial nad5 and cob Transcript Editing, Mitochondrion Biogenesis, and Maize Growth. Plant Cell 24: 676–691
Pubmed: Author and Title
Google Scholar: Author Only Title Only Author and Title

South PF, Cavanagh AP, Liu HW, Ort DR (2019) Synthetic glycolate metabolism pathways stimulate crop growth and productivity in the field. Science (80-) 363: eaat9077
Pubmed: Author and Title
Google Scholar: Author Only Title Only Author and Title

Stelpflug SC, Sekhon RS, Vaillancourt B, Hirsch CN, Buell CR, de Leon N, Kaeppler SM (2016) An expanded maize gene expression atlas based on RNA sequencing and its use to explore root development. Plant Genome. doi: 10.3835/plantgenome2015.04.0025
Pubmed: Author and Title
Google Scholar: Author Only Title Only Author and Title

Strand DD, Fisher N, Kramer DM (2017) The higher plant plastid NAD(P)H dehydrogenase-like complex (NDH) is a high efficiency proton pump that increases ATP production by cyclic electron flow. J Biol Chem 292: 11850–11860
Pubmed: Author and Title
Google Scholar: Author Only Title Only Author and Title

Sun F, Wang X, Bonnard G, Shen Y, Xiu Z, Li X, Gao D, Zhang Z, Tan BC (2015) Empty pericarp7 encodes a mitochondrial E-subgroup pentatricopeptide repeat protein that is required for ccmFN editing, mitochondrial function and seed development in maize. Plant J 84: 283–295
Pubmed: Author and Title
Google Scholar: Author Only Title Only Author and Title

Sun F, Xiu Z, Jiang R, Liu Y, Zhang X, Yang Y, Li X (2019) The mitochondrial pentatricopeptide repeat protein EMP12 is involved in the splicing of three nad2 introns and seed development in maize. J Exp Bot 70: 963–972
Pubmed: Author and Title
Google Scholar: Author Only Title Only Author and Title

Takabayashi A, Kishine M, Asada K, Endo T, Sato F (2005) Differential use of two cyclic electron flows around photosystem I for driving CO2-concentration mechanism in C4 photosynthesis. Proc Natl Acad Sci 102: 16898–16903
Pubmed: Author and Title
Google Scholar: Author Only Title Only Author and Title

Trapnell C, Roberts A, Goff L, Pertea G, Kim D, Kelley DR, Pimentel H, Salzberg SL, Rinn JL, Pachter L (2012) Differential gene and transcript expression analysis of RNA-seq experiments with TopHat and Cufflinks. Nat Protoc 7: 562–578
Pubmed: Author and Title
Google Scholar: Author Only Title Only Author and Title

Tsudzuki T, Wakasugi T, Sugiura M (2001) Comparative analysis of RNA editing sites in higher plant chloroplasts. J Mol Evol 53: 327–332
Pubmed: Author and Title
Google Scholar: Author Only Title Only Author and Title

Wang H, Nussbaum-Wagler T, Li B, Zhao Q, Vigouroux Y, Faller M, Bomblies K, Lukens L, Doebley JF (2005) The origin of the naked grains of maize. Nature 436: 714–719
Pubmed: Author and Title

Google Scholar: Author Only Title Only Author and Title

Wang H, Studer AJ, Zhao Q, Meeley R, Doebley JF (2015) Evidence that the origin of naked kernels during maize domestication was caused by a single amino acid substitution in tga1. Genetics 200: 965–974
Pubmed: Author and Title
Google Scholar: Author Only Title Only Author and Title

Wang P, Duan W, Takabayashi A, Endo T, Shikanai T, Ye J-Y, Mi H (2006) Chloroplastic NAD(P)H Dehydrogenase in Tobacco Leaves Functions in Alleviation of Oxidative Damage Caused by Temperature Stress. Plant Physiol 141: 465–474
Pubmed: Author and Title
Google Scholar: Author Only Title Only Author and Title

Wu A, Hammer GL, Doherty A, von Caemmerer S, Farquhar GD (2019) Quantifying impacts of enhancing photosynthesis on crop yield. Nat Plants 5: 380–388
Pubmed: Author and Title
Google Scholar: Author Only Title Only Author and Title

Xiu Z, Sun F, Shen Y, Zhang X, Jiang R, Bonnard G, Zhang J, Tan BC (2016) EMPTY PERICARP16 is required for mitochondrial nad2 intron 4 cis-splicing, complex i assembly and seed development in maize. Plant J 85: 507–519
Pubmed: Author and Title
Google Scholar: Author Only Title Only Author and Title

Xu F, Copeland C, Li X (2015) Protein Immunoprecipitation Using Nicotiana benthamiana Transient Expression System. Bio-protocol 5: e1520
Pubmed: Author and Title
Google Scholar: Author Only Title Only Author and Title

Yagi Y, Tachikawa M, Noguchi H, Satoh S, Obokata J, Nakamura T (2013) Pentatricopeptide repeat proteins involved in plant organellar RNA editing. RNA Biol 10: 1419–1425
Pubmed: Author and Title
Google Scholar: Author Only Title Only Author and Title

Yamori W, Makino A, Shikanai T (2016) A physiological role of cyclic electron transport around photosystem I in sustaining photosynthesis under fluctuating light in rice. Sci Rep 6: 1–12
Pubmed: Author and Title
Google Scholar: Author Only Title Only Author and Title

Yamori W, Shikanai T, Makino A (2015) Photosystem i cyclic electron flow via chloroplast NADH dehydrogenase-like complex performs a physiological role for photosynthesis at low light. Sci Rep 5: 13908
Pubmed: Author and Title
Google Scholar: Author Only Title Only Author and Title

Yang N, Liu J, Gao Q, Gui S, Chen L, Yang L, Huang J, Deng T, Luo J, He L, et al (2019) Genome assembly of a tropical maize inbred line provides insights into structural variation and crop improvement. Nat Genet 51: 1052–1059
Pubmed: Author and Title
Google Scholar: Author Only Title Only Author and Title

Yin X, Struik PC (2018) The energy budget in C4 photosynthesis: insights from a cell-type-specific electron transport model. New Phytol 218: 986–998
Pubmed: Author and Title
Google Scholar: Author Only Title Only Author and Title

Zhao L, Pan T, Cai C, Wang J, Wei C (2016) Application of whole sections of mature cereal seeds to visualize the morphology of endosperm cell and starch and the distribution of storage protein. J Cereal Sci 71: 19–27
Pubmed: Author and Title
Google Scholar: Author Only Title Only Author and Title